Untangling Illiquidity: Optimal Asset Allocation with Private Asset Classes

Daniel Dimitrov[*†]

November 25, 2025

Abstract

Strategic Asset Allocation in practice relies almost exclusively on mean – variance optimizations. This paper develops a dynamic portfolio choice model that embeds stochastic liquidity constraints into the SAA process. I show that ignoring asset illiquidity risk leads to systematic overallocation to private asset classes and exposes investors to severe consumption risk when liquidity shocks occur. Gains from investing in private assets are substantially tempered once illiquidity is accounted for. These results highlight the need to move beyond variance-only risk metrics and incorporate asset liquidity as a first-order consideration in the strategic portfolio design of investors considering private asset classes. In contrast to prior literature, which often adds complexity to the cash-flow modeling of illiquid assets but remains stylized in portfolio composition, I extend the framework to a realistic multi-asset universe and develop a fast numerical algorithm tailored for practical implementation.

JEL codes: D81,G11,G12,E21

Keywords: asset allocation, (il)liquidity, private assets, model misspecification

[*]De Nederlandsche Bank, University of Amsterdam; e-mail: d.k.dimitrov@uva.nl.

[†]I would like to thank Roel Beetsma and Dirk Broeders for extensive comments in earlier drafts of the paper; and Aleksandar Andonov, Matteo Bonetti, Damiaan Chen, Thierry Foucault, Frank de Jong (discussant), Reinier Goudswaard, Felix Kübler, Kostas Mavromatis, Bertrand Melenberg, Albert J. Menkveld, J.M. Schumacher, Christian Stoltenberg, Sweder van Wijnbergen, Bas Werker, and participants in the Market Microstructure Summer School 2021, MAF 2024, QFFE 2024, Netspar 2024 conferences for the valuable feedback and suggestions. The views expressed here are those of the author and do not reflect the views of De Nederlandsche Bank, or the Eurosystem. The code to reproduce the model presented in this paper is available at https://github.com/danielkdimitrov/portfolioChoiceIlliq.

1 Introduction

Strategic Asset Allocation (SAA) is the foundation of institutional portfolio management (Brennan et al., 1997; Campbell et al., 2004; Cochrane, 2022). Yet, in practice, the SAA process is dominated by legacy assumptions that fail to reflect the realities of modern institutional portfolios. Most institutions rely on (static) mean–variance optimization, developed under the implicit assumptions of continuous tradability of all assets and the full feasibility of allocation adjustments in the future (Kim et al., 2021; Begenau et al., 2025). While these assumptions are relatively innocuous for public equities and bonds, they are fundamentally flawed for private assets—such as private equity, private credit, real estate, and infrastructure—where invested capital can be locked up for years. Considering the growing popularity of private asset classes (Andonov et al., 2015, 2021, 2023; Broeders et al., 2021; Giesecke and Rauh, 2023; Begenau et al., 2025), this disconnect is particularly concerning. In this paper, I show that ignoring asset liquidity risk in the SAA leads to systematic overallocation to illiquid assets and exposes investors to severe consumption risk.

The academic literature on portfolio choice with liquidity frictions was developed precisely to address these challenges (e.g. Magill and Constantinides (1976); Longstaff (2001); Dai et al. (2011); Ang et al. (2014)). However, this literature remains highly stylized - complexity is developed around the nature of the friction and less so around the composition of the asset class investable universe. Similarly, the growing body of work on private equity allocation introduces complexity through detailed modeling of capital calls and distributions, yet still assumes a minimal liquid universe. While insightful, these models are difficult to scale to realistic multi-asset settings and thus have limited applicability for institutional SAA.

This paper addresses these limitations by developing a dynamic allocation framework that retains the tractability of a dynamic portfolio approach approach while accommo-

dating multiple asset classes. By simplifying the cash flow structure, the model becomes implementable for realistic SAA without sacrificing the essential economics of liquidity risk. Calibrating the model to forward-looking capital market assumptions, I quantify the welfare cost of ignoring illiquidity and show how optimal allocations differ from those implied by mean–variance optimization. The results underscore the need to move beyond variance-only risk metrics and incorporate liquidity as a first-order consideration in strategic portfolio design.

This paper is closely related to Ang et al. (2014), who study optimal allocation with one risky liquid and one illiquid asset under stochastic trading opportunities. I extend the theoretical dynamic model they propose to accommodate multiple assets and calibrate it on publicly available capital market assumptions (CMAs), I then solve for the optimal allocation to several private asset classes and quantify the welfare improvements they provide to an investor already holding a diversified liquid portfolio. Additionally, I evaluate the welfare losses associated with constructing a portfolio when liquidity risk is ignored. In doing so, I provide a fast and tractable numerical algorithm to solve the underlying dynamic optimization problem, thus demonstrating the model's practicality.

The paper also relates to several other strands of the investment literature. First, early studies such as Terhaar et al. (2003); Ilmanen et al. (2020) address illiquidity by emphasizing the need to unsmooth the historical returns of private asset classes, but stay the standard static mean–variance framework. My approach goes further by embedding illiquidity as an explicit risk factor in a dynamic optimization setting. The use of CMAs already embeds the return unsmoothing step allowing for forward-looking calibration using capital market assumptions.

Second, the extensive literature modeling private equity cash flows emphasizes the timing and uncertainty of capital calls and distributions, often at the expense of tractability for multi-asset allocation. Gourier et al. (2024) and Giommetti and Sorensen (2021) de-

veloped a cash-flow based dynamic model to examine the welfare implications of private equity capital commitments. Dimmock et al. (2023) suggest that the illiquidity of PE investments can be diversified through a dynamic strategy with staggered asset lock-up expirations, though this poses constraints for most investors, who typically hold only one or two PE managers (Gredil et al., 2020). Luxenberg et al. (2022) deviate from the dynamic programming formulation of the allocation problem and propose a model predictive control approach for solving it. Chen et al. (2025) propose a machine learning approach to solving the multi-dimensional dynamic problem that private equity investment entails. I abstract from detailed cash flow modeling with the private asset to focus on the first-order effect of liquidity restriction, while preserving scalability of the model to a realistic asset universe. This design bridges the gap between theoretical models and practical SAA implementation and allows evaluation of the welfare gains and losses associated with private assets in a more realistic portfolio setting.

Third, this paper builds on the dynamic portfolio choice tradition where infrequent trading creates a trade-off between diversification benefits and rebalancing constraints. This literature includes portfolio choice with trading costs (Zabel, 1973; Magill and Constantinides, 1976; Gennotte and Jung, 1994; Boyle and Lin, 1997; Dai et al., 2011), delayed execution (Longstaff, 2001), and inability to access the market in periods of deterministic (Miklós and Ádám, 2002; Dimmock et al., 2023) or, most closely related to the approach taken here, stochastic (Ang et al., 2014; Jansen and Werker, 2022) time length. Relative to this work—typically theoretical and stylized with one liquid and one illiquid asset—I retain the dynamic optimization approach but scale the liquid universe, which is essential for realistic SAA and for capturing substitution effects across liquid asset classes.

Liquidity in here arrives randomly through Poisson shocks, calibrated to the expected period over which the funds in the private asset classes are not redeemable. The uncertainty surrounding the timing of liquidity events affects the investor's optimal allocation

decision in several ways. In anticipation of prolonged periods of illiquidity for the private assets, it is optimal for the investor to preemptively reduce the portfolio consumption (withdrawal) rate and to tilt in advance the strategic asset weights away from the illiquid investment as a way of reducing the exposure to this additional source of risk. In addition, when the private asset has a publicly traded equivalent in the investment universe, a substitution effect is observed, by which the publicly traded substitute is preferred in the SAA instead of the private asset exposure.

I find that the attributes often cited as advantages of private assets — higher returns and diversification potential — are also the factors that interact negatively with illiquidity risk. Low correlation with the rest of the portfolio leads to a reduced possibility of hedging the volatility of the share in private illiquid assets. Consequently, the investor must secure additional risk-free buffers to mitigate the increased variability in portfolio consumption caused by fluctuations in the value of the private asset. This strategy ensures that negative shocks from publicly traded risky assets do not deplete liquidity and preserves consumption during periods when a large part of the investor's wealth is locked in illiquid allocations. A higher expected return of the private asset, on the other hand, due to the presence of illiquidity premia, leads to unintended overallocation through extended periods of illiquidity, as in expectation the share invested in the illiquid private asset rises above its SAA target.

Overall, I find that private equity, infrastructure investments, private real estate, and diversified hedge funds improve the Certainty Equivalent Consumption (CEC) of an optimizing investor with a CRRA utility who has a moderate risk appetite and already holds a diversified portfolio of stocks, bonds, and public real estate. Despite being economically substantial, these improvements are significantly tempered when illiquidity risk is taken into account. Yet, institutional investors widely use SAA optimization approaches that quantify risk purely from an asset volatility angle . Ignoring the liquidity aspects

of private assets thus exposes them to the risk of sub-optimal and overoptimistic allocation to private assets. Mimicking an investor who constructs her portfolio through a mean-variance lens without a view on illiquidity risk, I find a considerable welfare loss associated with the highly illiquid private asset classes: private equity, infrastructure, and real estate, and negligible loss for the relatively more liquid private asset classes, such as hedge funds.

A natural alternative to the one-step dynamic allocation developed in this paper is a decentralized "two-step" approach: first optimize within the liquid asset class to form a composite liquid portfolio, and then allocate between this composite and the illiquid asset following a stylized model with one liquid and one illiquid asset (e.g., Ang et al., 2014; Jansen and Werker, 2022). While this two-step structure may mirror a mandate-based investment processes, it is suboptimal when illiquidity hinders at the same time consumption, rebalancing, and cross-asset substitution in a non-separable way. In particular, the optimal composition within the liquid block generally depends on illiquidity risk—through state-dependent hedging demands and the value of rebalancing flexibility—and therefore cannot be optimized independently of the illiquid allocation. Relatedly, the literature on decentralized investment management shows that splitting decisions across mandates can entail large utility costs due to loss of diversification and misaligned horizons (Van Binsbergen et al., 2008). A one-step approach addresses these coordination failures directly by optimizing all liquid and illiquid positions jointly under the liquidity constraint.

The paper continues as follows: Section 2 outlines the model; Section 3 shows the key properties of the solution in a controlled stylized setting; Section 4 applies the model to analyst CMAs and evaluates the welfare benefits and misallocation costs associated with illiquid private assets; Annex A outlines the discretization steps and the numerical approach used to solve the presented dynamic portfolio choice model.

2 Model

The representative long-term investor in this model is infinitely lived and has a CRRA utility over the consumption amount C_t:

$$u(C_t) = \frac{C_t^{1-\gamma}}{1-\gamma} \tag{1}$$

with $t \geq 0$ as a time index, and $\gamma > 0, \gamma \neq 1$ as the coefficient of relative risk aversion, where higher γ implies a higher risk aversion. The investor constructs a portfolio of risky assets, out of which consumption is funded (no other intermediate income is available).

The investment universe: The instantaneous risk-free rate is fixed. Denoting it as r, the price B_t of a risk-free asset then follows the process:

$$dB_t/B_t = rdt \tag{2}$$

In addition, there are n marketable risky assets. The vector of their returns $\boldsymbol{dS/S}$ evolves as a multivariate Geometric Brownian Motion process such that:

$$\frac{\boldsymbol{dS}_t}{\boldsymbol{S}_t} = \boldsymbol{\mu}dt + \boldsymbol{\sigma}\boldsymbol{dZ}_t \tag{3}$$

where $\mathbb{1}$ stands for a n-dimensional column vector of ones, $\boldsymbol{dZ}_t$ is a vector of n independent Brownian motions supported by probability space $(\Omega, \Im, \mathbb{P})$; $\boldsymbol{\mu}$ is a $n \times 1$ vector of expected returns; $\boldsymbol{\sigma}$ is $n \times n$ lower triangular matrix holding the sensitivities of the risky asset returns to the Brownian uncertainties with $\boldsymbol{\Sigma} = \boldsymbol{\sigma}\boldsymbol{\sigma}'$ representing the corresponding variance-covariance matrix; $\boldsymbol{\lambda} = \boldsymbol{\sigma}^{-1}(\boldsymbol{\mu} - r\mathbb{1})$ is the price of risk.

Introducing the illiquid private asset: Assume now that the asset corresponding to the n-th row in the vector specification (3) is not marketable all the time. A market opportunity for it arises only when a Poisson process N_t with intensity η hits. The Poisson process is independent of the Brownian motions defined earlier.[1]

To keep track of liquid and illiquid assets, we define the partitioned vector of expected asset returns and the partitioned matrix of sensitivities to the respective Brownian motions driving asset volatility:

$$\boldsymbol{\mu} = \begin{bmatrix} \boldsymbol{\mu}_w \\ \mu_x \end{bmatrix}, \boldsymbol{\sigma} = \begin{bmatrix} \boldsymbol{\sigma}_w \\ \boldsymbol{\sigma}_x \end{bmatrix} \tag{4}$$

where $\boldsymbol{\mu}_w$ is a $(n-1) \times 1$ vector that captures the expected return of the liquid assets; μ_x is the drift of the illiquid asset; $\boldsymbol{\sigma}_w$ and $\boldsymbol{\sigma}_x$ are respectively $(n-1) \times n$ and $1 \times n$ matrices that capture the sensitivities respectively of the liquid assets and the illiquid asset to the Brownian motions.

Interpretation of the Liquidity Event: The implications of the liquidity events in this model are worth discussing before proceeding. The model assumes that the illiquid asset can only be traded at random times, modeled as an exogenous Poisson process. This abstraction is standard in the academic literature on portfolio choice with illiquidity and is consistent with the benchmark model of Ang et al. (2014). My interpretation of these liquidity events in the case of private asset classes is intentionally broad: they can represent natural redemption opportunities, the closing of a fund, or the sporadic availability of a secondary market transaction. For tractability, the timing of these events is not endogenized, but treated as exogenous and infrequent.

[1] Also, in the limit, when $1/\eta \to 0$, the private asset approaches full liquidity, and (as we will see later) the solution of the optimal investment problem will resemble the Merton portfolio choice model. On the other hand, as $1/\eta \to \infty$, the private asset is never liquid, and the solution will converge to a Merton portfolio choice problem in which the private asset is completely excluded from the investment universe.

This modeling choice is appropriate for many private asset contexts where liquidity is uncertain and costly. Examples include venture capital or private equity fund stakes with limited secondary activity, infrastructure funds held to maturity, or illiquid real estate and bespoke credit vehicles with no reliable exit market. In these cases, secondary markets either do not exist or are so thin and price-depressed that trading is effectively rare and costly (Gourier et al., 2024). Modeling illiquidity as an exogenous Poisson arrival of trading opportunities therefore provides a conservative and realistic representation of liquidity risk at the strategic allocation stage.

It is important to clarify that the model does not rule out secondary markets; rather, it captures their sporadic and uncertain nature through the stochastic liquidity arrival process. What the model abstracts from for tractability is endogenizing the decision to tap into the secondary market. Incorporating such features is an interesting extension for future research (see, e.g., Bollen and Sensoy, 2022; Gourier et al., 2024). From the perspective of SAA, where allocations are determined before specific managers or mandates are selected (Brennan et al., 1997; Martellini and Milhau, 2020), it is reasonable to assume that liquidity opportunities are uncertain and cannot be relied upon for planning purposes.

Finally, by construction, arrivals of the liquidity opportunities embedded in the Poisson structure are $i.i.d$ over time. While this is problematic over very short horizons in which clustering, autocorrelation or liquidity spillover effects may be present, these are less likely to play a role for long-term investors. A second implicit simplification in this model is to assume that even though the private asset is illiquid, the investor can continuously observe the evolution of its value over time, and when the exogenous Poisson shock hits, the investor is able to realize this value. While in reality information frictions may be present on a manager level (Sefiloglu, 2022), such complications are typically outside the scope of a strategic asset allocation problem. The SAA by design ignores manager

level frictions and focuses on aggregate asset classes, assuming that the risk and return parameters of the model once calibrated to the CMAs will already account for any losses due to manager-level frictions.

2.1 Model Dynamics with One Illiquid Asset

The investor's total portfolio wealth Q_t can be split into liquid wealth W_t, invested in risky and riskless assets, and illiquid wealth X_t, invested in the illiquid private asset. The only income the investor receives is from the capital gains on the invested wealth. In line with the literature and empirics, the illiquid asset cannot be used as collateral, and as a result, illiquidity cannot be circumvented by pledging the asset and issuing debt instead. The investor controls the asset allocation first through the liquid portfolio composition, defined by the allocation vector $\boldsymbol{\theta}_t$ into liquid risky assets (fractions defined as proportions from liquid wealth); and second, through the transfers dI_t between liquid and illiquid wealth, which are possible only when the Poisson shock hits. The investor can consume directly only out of liquid wealth, so we define the consumption rate as a fraction of liquid wealth: $c_t = \frac{C_t}{W_t}$.

We can write the wealth dynamics of liquid and illiquid wealth as follows:

$$\begin{aligned} dW_t/W_t &= (r + \boldsymbol{\theta}_t'(\boldsymbol{\mu}_w - r\mathbb{1}) - c_t)dt + \boldsymbol{\theta}_t'\boldsymbol{\sigma}_w \boldsymbol{dZ}_t - dI_t/W_t \\ dX_t/X_t &= \mu_x dt + \boldsymbol{\sigma}_x \boldsymbol{dZ}_t + dI_t/X_t \end{aligned} \tag{5}$$

Naturally, then we have $dQ_t = dW_t + dX_t$.

The value function subject to these wealth dynamics can then be written as

$$V(W_t, X_t) = \sup_{\theta_s, dI_s, c_s} E_t \int_t^\infty \mathrm{e}^{-\beta(s-t)} u(C_s) ds \tag{6}$$

which yields the HJB equation:

$$\begin{aligned}
&\mathcal{L}^C + \mathcal{L}^\theta + \mathcal{L} + \eta\left(V^* - V(W_t, X_t)\right) - \beta V(W_t, X_t) = 0 \text{ where} \\
&\mathcal{L}^C = \sup_{C_t}\left\{u(C_t) - C_t V_W\right\} \\
&\mathcal{L}^\theta = \sup_{\theta_t}\left\{(r + \boldsymbol{\theta}_t'(\boldsymbol{\mu}_w - r\mathbb{1})V_W W_t + \frac{1}{2}V_{WW}W_t^2\boldsymbol{\theta}_t'\boldsymbol{\sigma}_w\boldsymbol{\sigma}_w'\boldsymbol{\theta}_t + V_{WX}W_tX_t\boldsymbol{\theta}_t'\boldsymbol{\sigma}_w\boldsymbol{\sigma}_x'\right\} \\
&\mathcal{L}^X = V_X\mu_x + \frac{1}{2}V_{XX}X^2\boldsymbol{\sigma}_x\boldsymbol{\sigma}_x'
\end{aligned} \tag{7}$$

Now, following Ang et al. (2014), denote the realized allocation to the private illiquid asset as: $\xi_t = \frac{X_t}{Q_t}$. Using the homogeneity property of the value function under a CRRA utility, we can factor out total wealth and define a reduced value function as:

$$H(\xi) \equiv V((1-\xi), \xi) = \left(\frac{1}{Q_t}\right)^{1-\gamma} V(W_t, X_t) \tag{8}$$

where $H(\xi_t)$ is a finite, continuous and concave function, maximized at ξ^* for $\xi \in [0, 1)$.

By design, consumption in the periods between the Poisson liquidity arrivals can be funded from liquid wealth only, so by maximizing $\mathcal{L}^C$ we we can show optimal consumption c_t depends only on the share of the illiquid private asset, the reduced value function and its derivative as

$$c(\xi_t) = \left((1-\gamma)H(\xi_t) - H'(\xi_t)\xi_t\right)^{-\frac{1}{\gamma}}(1-\xi_t)^{-1} \tag{9}$$

In contrast to the fixed Merton optimal consumption rate in (26), the consumption rate between trading events now it is state-dependent, varying with ξ_t.

The optimal investment in the risky liquid asset can be derived from (7) also as a

reaction function to the illiquid wealth share in the portfolio:

$$\boldsymbol{\theta}(\xi_t) = \underbrace{\left(\boldsymbol{\sigma}_w \boldsymbol{\sigma}_w'\right)^{-1} \left(\boldsymbol{\mu}_w - r\mathbb{1}\right) \underbrace{\left(-\frac{V_W}{V_{WW} W_t}\right)}_{\Phi(\xi_t)}}_{\text{Investment Demand}} + \underbrace{\left(\boldsymbol{\sigma}_w \boldsymbol{\sigma}_w'\right)^{-1} \boldsymbol{\sigma}_w \boldsymbol{\sigma}_x' \underbrace{\left(-\frac{V_{WX} X_t}{V_{WW} W_t}\right)}_{\Psi(\xi_t)}}_{\text{Hedging Demand}} \tag{10}$$

The allocation to liquid risky assets can thus be split into two parts. First is the *investment demand* term is proportional to each liquid asset's price of risk and the investor's effective risk tolerance $\Phi(\xi_t)$. The *hedging demand* term arises from the investor's desire to offset shocks to the illiquid asset through exposure to correlated liquid assets. The term $\Psi(\xi_t) \leq 0$ under standard concavity assumptions, so the sign of the correlation determines whether the hedging demand increases or decreases exposure to liquid risk.[2]

Whenever liquidity is available, the investor has the freedom to move to the portfolio's optimal strategic allocation in the illiquid private asset. Formally, this implies moving to the maximum of the reduced value function $H(\xi_t)$.[3] As a result, we have the strategic allocation to the illiquid private asset defined as:

$$\xi^* = arg \max_{\xi} H(\xi) \tag{11}$$

Then, factoring out total wealth from each term in (7), we obtain a reduced-form version

[2]See Annex C.2 for analytical details into these terms. To gain intuition into the hedging and the investment terms of the allocation problem, we can simplify the problem and look at a three-asset case with a liquid risk-free asset, liquid public equity, and an illiquid private asset (the original set-up of Ang et al. (2014)):

$$\boldsymbol{\mu} = \left[\mu_1, \mu_2\right]^\intercal, \boldsymbol{\sigma} = \begin{bmatrix} \sigma_1 & 0 \\ \rho\sigma_2 & \sqrt{1-\rho^2}\sigma_2 \end{bmatrix}, \boldsymbol{\Sigma} = \begin{bmatrix} \sigma_1^2 & \rho\sigma_1\sigma_2 \\ \rho\sigma_1\sigma_2 & \sigma_2^2 \end{bmatrix}$$

The *investment demand* in the liquid risky asset then is given by: $\frac{\mu_1 - r}{\sigma_1^2}\Phi(\xi_t)$. The *hedging demand* term is represented by: $\frac{\sigma_2 \rho}{\sigma_1}\Psi(\xi_t)$.

[3]This is equivalent to choosing an optimal transfer amount $dI_\tau = (\xi^* - \xi_{\tau^-})W_{\tau^-}$ where ξ_{τ^-} is the illiquid asset allocation immediately before rebalancing occurs.

of the HJB equation as:

$$\mathcal{L}^C(\xi) + \mathcal{L}^\theta(\xi) + \mathcal{L}(\xi) + \eta\left(H^* - H(\xi)\right) - \beta H(\xi) = 0 \tag{12}$$

where each term depends only on ξ, its derivatives, and the model parameters. The original problem of solving the HJB equation for $V(W_t, X_t)$ has thus been reduced to solving simultaneously for the reduced value function $H(\xi_t)$ and its maximizing point ξ^*.

Intuitively, when the asset remains illiquid, the investor cannot withdraw from or contribute to illiquid wealth, preventing the portfolio from rebalancing to the strategic allocation target of ξ^*. Between Poisson events, first, continuous consumption will drain liquid wealth and increase the share of illiquid assets; and second, the share of the illiquid private asset fluctuates stochastically with the realized dynamics of the prices of the assets in the portfolio. The illiquid allocation with a liquidity event ξ^* and its corresponding allocation of the liquid risky assets $\boldsymbol{\theta}(\xi^*)$ represent the base strategic allocations to which the investor returns whenever the Poisson shock allows. This will define the SAA allocation. In periods of illiquidity, when the allocation to the illiquid asset cannot be adjusted, $\theta(\xi_t)$ will represent the optimal tactical allocation to liquid risky assets as a reaction to the uncontrolled movements in the share of the private asset. The exact functional form of the tactical allocation function will be determined numerically.

2.2 Certainty equivalent consumption:

Apart from determining the optimal investment and consumption strategies, one additional goal is to compare different investment strategies in utility-equivalent terms. For this purpose, define the lifetime utility value generated by guaranteed continuous consumption stream CEC_t (standing for the certainty equivalent consumption) fixed at time

t as:

$$\int_t^{\infty} \mathrm{e}^{-\beta s} u(CEC_t) ds = \frac{1}{\beta} u(CEC_t)$$

The CEC consumption stream then is what makes the investor indifferent between the risk-free stream CEC_t and the risky consumption stream underlying a particular investment strategy, so we get:

$$CEC_t \equiv I_u \left(\beta E_t \int_t^{\infty} \mathrm{e}^{-\beta s} u(C_s) ds \right) \tag{13}$$

where $I_u(.)$ stands for the inverse of the utility function. We can then use the value function from each dynamic investment strategy to value the CEC associated with it. For example, we find that, for the Merton case with consumption rate c_M (see Annex B.1), the CEC per unit of total wealth is:

$$CEC_M = \beta^{\frac{1}{1-\gamma}} \left(\frac{1}{c_M} \right)^{\frac{1}{1-\gamma}}$$

For the illiquid case, the CEC (per unit of total wealth) will depend on the current share of illiquid wealth:

$$CEC_t(\xi) = (\beta(1-\gamma)H(\xi_t))^{\frac{1}{1-\gamma}} \tag{14}$$

3 Comparative statics of the private asset allocation

This section examines the model solution properties under a controlled setting which disentangles the effects coming solely from illiquidity risk by varying the intensity of the Poisson process governing the illiquidity risk and keeping all other properties of the

risky assets the same. I consider an investment universe containing a risk-free asset and three risky assets with the same variance and expected return profile. One of the risky assets is not publicly traded and thus is subject to illiquidity risk. In line with the model of illiquidity from Section 2, its allocation can, on average, be adjusted once every $1/\eta$ years. The two liquid risky assets capture the comparative statics of different correlations between the liquid and the illiquid assets and examine the strength of the substitution effect when the illiquidity parameter intensifies.

There are two key assumptions in the baseline case: the private asset does not carry an illiquidity premium, and it is assumed to be uncorrelated to the liquid public assets. Table 1 provides a summary of all the model inputs. The choice for expected return and standard deviation is consistent with the profile of Large Cap US Equity, and the risk-free rate is aligned with the expected return on Money Market funds in the JP Morgan long-term CMAs for 2025 (discussed in detail in Section (4)). The private asset, unless specified otherwise, trades with an intensity of $\eta = 1/10$, implying ability to rebalance back to the target SAA approximately on average once every ten years in the long run. The coefficient of relative risk aversion is set to $\gamma = 6$. This parameterization results in moderately aggressive portfolios - for instance, in the Merton model, the optimizing investor allocates approximately 70% to risky assets (equally distributed between the risky assets) and 30% to the risk-free asset.

There is a debate regarding the size of the liquidity premium and the correlations between private and traditional asset classes. The oversmoothed observed returns tend to overstate private asset performance (Terhaar et al., 2003), making the estimation of the illiquidity premium they bear a difficult task (Ang et al., 2018; Franzoni et al., 2012). In addition, metrics like IRR commonly reported by private funds, complicate comparisons with public equity equivalents and can be manipulated by private fund managers. Also, performance assessment is hampered by infrequent valuations, selection bias (as funds

typically trade when successful), and reporting bias (with better-performing funds more likely to disclose their results).

Due to the ambiguity on these parameters, I conduct a comparative statics analysis with respect to illiquidity premium in the private asset and its correlation with the liquid assets in the investment universe. Thus, I evaluate the model when the illiquid asset bears a liquidity premium of 3% in line with estimates by Franzoni et al. (2012), deviating from zero percent premium in the baseline case; and when it has 80% correlation with one of the liquid assets (labeled Public 2), inspired by Franzoni et al. (2012); Ang et al. (2018); Ang and Sorensen (2012) who find that private and public equity are highly correlated and exposed to the same underlying risk factors.

Table 1: Baseline parametrization

Parameter	**Definition**	**Default Value**
r	risk-free rate	3.1%
β	personal discount rate	3.1%
$\mu_1 = \mu_2 = \mu_3$	risky assets expected return	6.7%
$\sigma_1 = \sigma_2 = \sigma_3$	risky assets volatility	16.2%
ρ	correlation between public asset 2 and the private asset	0 or 0.80
lp	illiquidity premium of the private asset on top of μ_3	0% or 3%
$1/\eta$	average time (in years) between a trading opportunity arises	10
γ	risk aversion parameter in the CRRA utility function	6

Note. The table shows the baseline parameter values used for the comparative statics exercise.

The Value Function: The blue surface in Figure 1a shows the shape of the investor's reduced value function $H(\xi)$ and illustrates its sensitivity to the severity of the private asset illiquidity.[4] A higher $1/\eta$ implies longer expected waiting times before the investor can adjust the allocation of the private asset back to its SAA.

[4]The value function is derived numerically. See the value function iteration and quadrature algorithms described in Annex A.

As the expected waiting time increases, the maximum of the value function shifts toward lower allocations to the illiquid private asset ξ, as indicated by the red curve on the surface. This reflects the investor's desire to reduce the strategic allocation to the private asset. For example, when the expected waiting time is 1 year, the optimal allocation to the private asset is 21%. This allocation, however, declines to 5.9% when the waiting time extends to 15 years, reflecting the investor's desire to mitigate illiquidity risk already in the portfolio construction phase.

With higher illiquidity, the value function exhibits greater curvature over the realized allocation of the private asset. As indicated in Equations (9) and (10) this curvature plays a role in the liquid asset allocation and in the consumption rate adjustments during the periods in which liquidity is not available. With longer waiting times, as the realized private asset allocation drifts away from the strategic target, the tactical adjustments become more prominent, and the consumption rate and the risky allocations are reduced even with mild deviations of ξ above the strategic target. This effect is illustrated in Figures 1c and 1b.

The shape of the value function also indicates how sensitive investor welfare is with respect to the portfolio share locked up in the private asset. The concavity of the value function implies that under-investing in the private asset would lead to a loss of investor welfare, as a potential source of diversification or return has been underappreciated. At the same time, overallocating would also lead to a loss, as the investor bears more illiquidity risk than is optimal according to their risk preferences. The steeper slope of the value function shows that overallocating to the private asset is having an increasingly negative impact on investor welfare when with higher illiquidity.

Strategic Asset Allocation: Table 2 shows further how the overall strategic portfolio allocations are affected by the severity of the liquidity friction, considering the four cases for the parametrization of the private asset: with and without a liquidity premium, with

Figure 1: Optimal Solution

(a) Value Function, $-\ln(-H(\xi))$

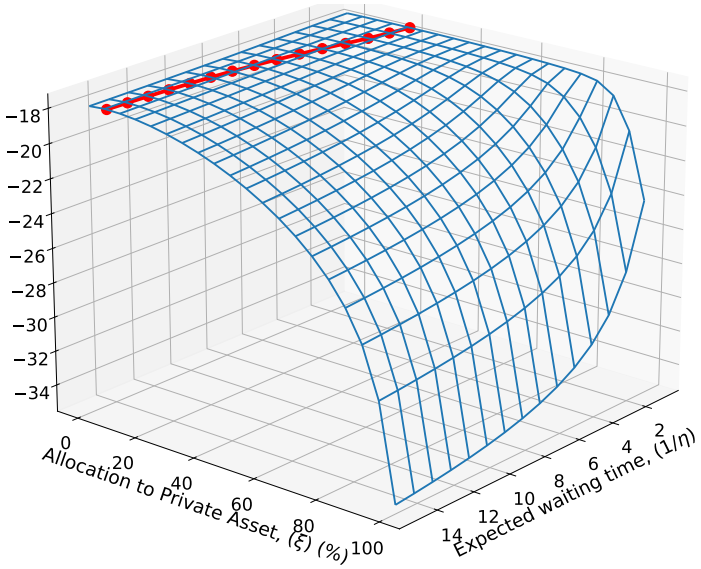

(b) Consumption

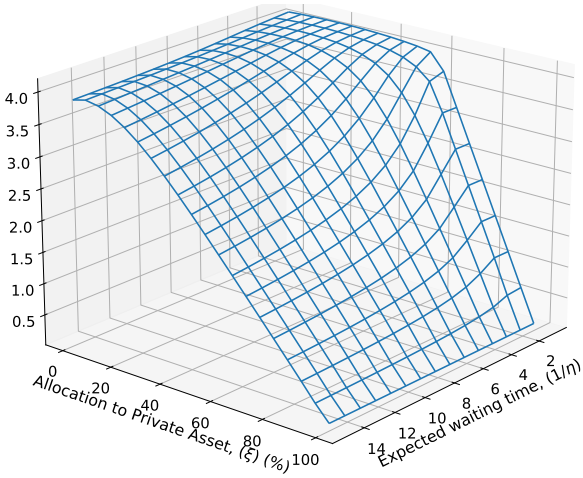

(c) Liquid Risky Alloc.

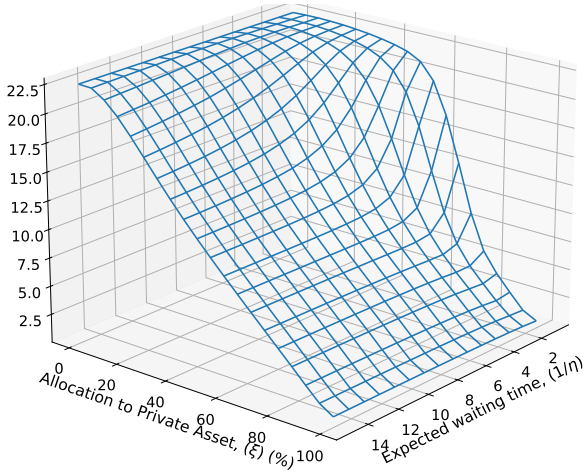

Note. This figure shows the reduced value function sensitivity to the share ξ of the private asset in the portfolio for the different severity of trading friction, $1/\eta$. The red curve on top of the surface highlights the optimizing strategic allocation to the private asset at each level of illiquidity. Panels (b) and (c) show respectively the optimal consumption rate and the the optimal allocation to one of the liquid risky assets (both as % of the total portfolio).

and without correlation to a public asset from the investment universe. Each table first shows the Merton solution with the full investment universe (row '3m'), hypothesizing that the private asset can always be traded, and the Merton solution only with the two publicly traded assets and cash (row '2m'), hypothesizing that the private asset is excluded from the investment universe. The '2m' case thus serves as a basis for evaluating the improvement in CEC terms of including a private asset in the portfolio. The '3m' provides a ceiling on maximum achievable CEC if the the private asset were fully liquid. The model with illiquidity converges to the '3m' case when the Poisson intensity η is large and converge to the '2m' case when it is small, implying large waiting times between opportunities to rebalance the private asset allocation.

Table 2a looks at a case when the private asset has high diversification potential, i.e. zero correlation to the two public assets. When trading can occur up to a year on average, the optimal allocation with illiquidity is still close to the continuous trading optimal allocation (row '3m') of 22.69%. As the trading friction intensifies, however, the allocation to the private asset is significantly reduced, down to 5.95% with 15 years average waiting time. Overall, this shift becomes economically significant when the average waiting time is above 2 years. In this baseline case, the reduction in the private asset allocation is not in favor of liquid risky assets, but rather in favor of building stronger cash buffers. This ensures that with prolonged periods of illiquidity the volatility of the public assets will not drain total liquidity from the portfolio, and the investor can still keep robust consumption until the next rebalancing opportunity arrives.

When the private asset is correlated to a public asset, Public 2 in Table 2b, a **substitution effect** appears - the liquid risky asset displaces the allocation to the correlated private asset. Public asset 2, which is 80% correlated, serves as an effective substitute when the illiquidity in the public asset intensifies. As the diversification benefits in this case are small, we can see that despite the significant relocation from the private asset

Table 2: Strategic Asset Allocation with a Private Asset

(a) High Diversification ($\rho = 0; lp = 0$)

$1/\eta$	Cash	Public 1	Public 2	Private	CEC
3m	31.92	22.69	22.69	22.69	4.36
0.5	32.77	22.52	22.52	22.19	4.35
1	33.38	22.51	22.51	21.59	4.34
2	34.51	22.49	22.49	20.50	4.33
5	39.60	22.45	22.45	15.50	4.28
10	46.41	22.49	22.49	8.62	4.16
15	49.09	22.49	22.48	5.94	4.09
2m	54.61	22.69	22.69	-	3.93

(b) Low Diversification ($\rho = 0.8; lp = 0$)

$1/\eta$	Cash	Public 1	Public 2	Private	CEC
3m	52.09	22.69	12.61	12.61	3.98
0.5	52.38	22.58	12.72	12.33	3.97
1	52.43	22.58	12.96	12.03	3.97
2	52.56	22.57	13.48	11.39	3.97
5	53.04	22.57	15.52	8.86	3.96
10	53.82	22.57	18.7	4.9	3.95
15	54.22	22.57	20.29	2.92	3.94
2m	54.61	22.69	22.69	-	3.93

(c) High Diversification, Premium ($\rho = 0; lp = 0.03$)

$1/\eta$	Cash	Public 1	Public 2	Private	CEC
3m	13.01	22.69	22.69	41.61	5.40
0.5	14.83	22.38	22.38	40.41	5.37
1	15.95	22.34	22.34	39.37	5.36
2	20.56	22.24	22.24	34.96	5.30
5	35.24	22.20	22.20	20.35	4.91
10	43.70	22.33	22.33	11.64	4.55
15	47.27	22.48	22.48	7.78	4.39
2m	54.61	22.69	22.69	-	3.93

(d) Low Diversification, Premium ($\rho = 0.8; lp = 0.03$)

$1/\eta$	Cash	Public 1	Public 2	Private	CEC
3m	41.58	22.69	(29.42)	65.14	5.23
0.5	42.45	22.41	(28.15)	63.29	5.20
1	42.70	22.36	(26.52)	61.46	5.19
2	43.41	22.29	(22.75)	57.05	5.16
5	49.29	22.24	2.92	25.55	4.67
10	51.47	22.33	11.15	15.06	4.39
15	52.52	22.43	14.55	10.50	4.27
2m	54.61	22.69	22.69	-	3.93

Note. This table shows the optimal SAA weights and Certainty Equivalent Consumption (CEC) as a function of the expected waiting time ($1/\eta$, in years) to trade the illiquid asset. The rows $2m$ and $3m$ stand for the continuous-trading Merton case with two and three risky assets, respectively. All numbers are in percentages from total investor wealth.

into Public 2, the CEC losses are not significant, and CEC consumption stays around 3.9% in all cases. In contrast to the diversifying case, however, now cash buffers were already high even when the private asset was fully liquid. The high buffers protect against the individual asset volatility which cannot be dampened in the portfolio through diversification.

Consider the case when the illiquid asset bears a liquidity premium (Tables 2c and 2d). First, when the private asset allocation can be rebalanced relatively frequently (less than 2 years on average) and a well-correlated publicly traded equivalent exists (Public 2 in Table 2d), the investor sells short the public equivalent and allocates the proceeds to

the illiquid private asset. This exploits the opportunity to harvest the illiquidity premia of the private asset while also hedging its volatility through the short position in its public equivalent. However, as the time to trade the illiquid asset extends beyond five years, this strategy becomes suboptimal, and the investor transitions to a long-only portfolio. The optimal allocation still amounts to about 10% in the private asset when illiquidity is extremely low, indicating an ability of the investor to still accommodate the illiquidity risk associated with the private asset. Note that in this case the substitution effect observed earlier now works in reverse - the investor prefers the higher yielding private asset and allocates less to Public 2 compared to the case when the illiquid asset has zero correlation with it.

The Distribution of the ξ and Denominator-Effect Implications: The dynamics of the illiquid private asset share ξ over time are driven by several forces. While the investor can return to the optimal SAA levels ξ^* when a liquidity opportunity arises, the rest of the time the realized allocation drifts freely based on the how the value of the liquid sub-portfolio changes relative to the value of the illiquid allocation. This corresponds to the denominator (over-allocation) effect, observed in practice: when the illiquid asset cannot be traded, the liquid share ξ compresses mechanically as public markets decline by more than private markets, and as consumption is financed out of liquid wealth. The implied illiquid weight then drifts above its strategic target, even when the investor does nothing. Unless a liquidity event arrives, the investor most of the time cannot control the allocation of the private asset.

Figure 2a shows a density plot of the realized ξ for a simulated time path of the optimal investment portfolio under the baseline case. In both the five-year and the 15-year liquidity waiting time, most of the distribution mass of the realized allocation is concentrated just above the SAA value ξ^* indicated by the vertical dotted line. As expected, in the 15-year waiting time, the optimal SAA to the private asset decreases. At the same

time, the right tail of the realized allocation to the private asset becomes fatter, indicating that while the investor has preemptively reduced the strategic allocation to the private asset compared to the more liquid case, there is still a growing likelihood of extreme unintended over-allocation to the private asset. Figure 2b further shows that the tendency for over-allocation becomes particularly pronounced when the private asset carries a high liquidity premium. Especially in the 15-year case, the median realized allocation to private assets is clearly above the strategic level (the dotted vertical line at ξ^*), reflecting the persistent drift in ξ caused by the prolonged illiquidity periods and the tendency for outperformance of the illiquid asset. This is the model's analogue of the denominator effect: liquid valuations fall quickly, and illiquidity prevents timely rebalancing, causing the private sleeve to dominate the portfolio share for extended periods. The simulated distribution of ξ thus provides model-based guidance on how often and how far private allocations can deviate from SAA targets when illiquidity binds, and for how long those deviations persist.

Figure 2: The Density of Realized Private Asset Allocation

(a) No Liquidity Premium (b) With Liquidity Premium

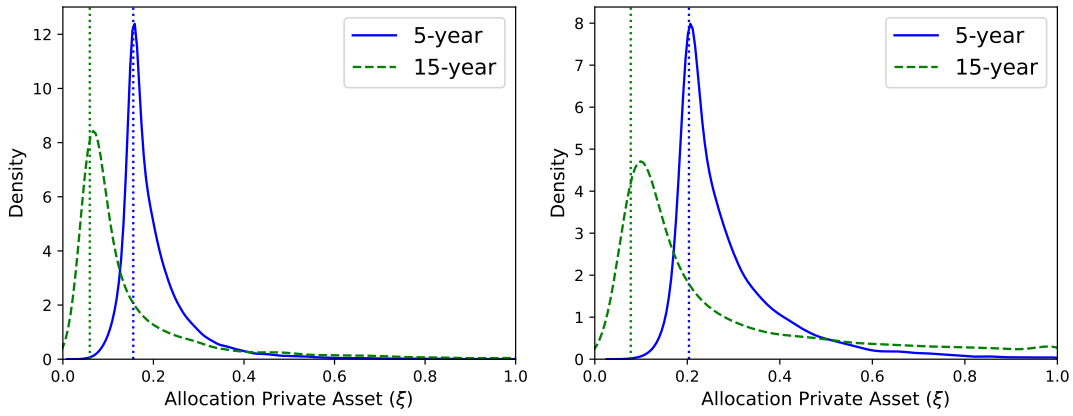

Note. Figures (a) and (b) show kernel plots of the realized allocation to the private asset without and respectively with an illiquidity premium for the private asset. The vertical dotted lines indicate the strategic allocation, ξ^*. The results are based on model simulation.

Optimal consumption and illiquidity-related consumption variability: Table 3 highlights how illiquidity risk impacts the realized allocation of the private asset and the realized consumption rate. The table shows a 95% range in a model simulation for the consumption rate and for private asset allocation, when the expected waiting time between Poisson shocks is varied. To put the risk of illiquidity in perspective, the numbers in bold show cases in which the realized consumption falls below the benchmark Merton optimal consumption of 3.78% evaluated when the private assets are excluded from the investment universe. As the waiting time of liquidity increases above two years, reasonable tail scenarios appear in which the investor needs to significantly curb consumption due to portfolio liquidity dry-ups. This risk of over-allocating to the private asset and consequently experiencing a liquidity dry-up becomes particularly notable with prolonged expected waiting times between rebalancing opportunities combined with an illiquidity premium on the private asset (tables 3c and 3d). In those cases, we observe that the 97.5 percentiles of the realized private asset allocation increase substantially. The risk appears that the private asset may dominate the whole portfolio without the investor being able to rebalance back to the strategic targets.

Next, I compare the consumption rate with an illiquid private asset (solid blue curve in Figure 3) against the consumption rate without it (lower dotted line, derived from the Merton Model), and the consumption rate assuming, hypothetically, that the private asset is fully liquid (upper dashed line, also derived via the Merton Model). The gap between the two horizontal lines shows the overall potential for consumption improvement from the private asset. As can be expected, the potential to improve consumption is higher when the private asset offers stronger diversification potential, as in Figure 3a, or when it embeds an illiquidity premium, as illustrated in Figures 3c and 3d. Conversely, Figure 3b demonstrates that a high correlation between the liquid and illiquid assets significantly limits this potential. In the cases when strong improvement potential exists, the presence

Table 3: Private Asset SAA and Consumption Rate, 95% Range of Realized Scenarios

(a) $\rho = 0; lp = 0$

	Allocation, ξ			Consumption Rate		
$1/\eta$	2.5%	50%	97.5%	2.5%	50%	97.5%
0.5	19.14	22.19	27.13	4.12	4.12	4.12
1	17.75	21.59	30.18	4.11	4.12	4.12
2	15.62	20.74	35.05	4.08	4.11	4.11
5	11.09	17.60	46.18	**3.59**	4.06	4.07
10	5.75	11.21	56.83	**2.42**	3.96	3.97
15	3.64	8.46	61.26	**1.97**	3.90	3.92

(b) $\rho = 0.8; lp = 0$

	Allocation, ξ			Consumption Rate		
$1/\eta$	2.5%	50%	97.5%	2.5%	50%	97.5%
0.5	10.75	12.33	15.11	3.82	3.82	3.82
1	9.98	12.03	16.9	3.82	3.82	3.82
2	8.9	11.61	19.65	3.82	3.82	3.82
5	6.27	9.96	27.37	**3.76**	3.81	3.82
10	3.59	6.45	36.92	**3.29**	3.80	3.80
15	2.08	4.38	42.92	**2.81**	3.79	3.80

(c) $\rho = 0.8; lp = 0.03$

	Allocation, ξ			Consumption Rate		
$1/\eta$	2.5%	50%	97.5%	2.5%	50%	97.5%
0.5	36.85	40.41	48.72	4.91	4.91	4.91
1	34.84	39.37	54.33	4.88	4.90	4.91
2	29.82	36.92	60.99	4.54	4.86	4.86
5	16.33	24.83	70.70	**2.50**	4.54	4.57
10	9.10	18.32	87.57	**0.99**	4.21	4.28
15	6.31	15.09	93.95	**0.52**	4.08	4.16

(d) $\rho = 0.8; lp = 0.03$

	Allocation, ξ			Consumption Rate		
$1/\eta$	2.5%	50%	97.5%	2.5%	50%	97.5%
0.5	58.05	63.29	76.19	4.76	4.78	4.81
1	54.16	61.46	84.10	4.64	4.77	4.83
2	48.62	60.28	93.18	4.26	4.75	5.00
5	22.17	31.91	83.99	**2.23**	4.34	4.37
10	13.17	24.56	94.69	**1.09**	4.07	4.15
15	9.41	19.78	98.64	**0.84**	3.97	4.06

Note. This table shows the realized private asset allocations (q values) and consumption rates as a function of the expected waiting time ($1/\eta$, in years) to trade the illiquid asset. The columns $q = 2.5\%$, $q = 50\%$, and $q = 97.5\%$ indicate the quantiles of the respective variables. The numbers in bold show the cases in which the realized consumption falls below the Merton optimal consumption of 3.78% when the private asset is excluded. All numbers are in percentages from total investor wealth.

of illiquidity prevents the full realization of this potential as with higher share of the private asset, the investor has to curb consumption. This is captured by the downward-sloping curve in the right section of the charts. Since illiquidity introduces consumption dependence on the realized private asset holdings, as the realized allocation to the private asset drifts above the strategic optimum, the investor will need to adjust downward the consumption rate below its potential (the diamond at the top of the curve). The shaded grey areas in the figure then show the 95% range of realized consumption rates in a simulated model run. In this line of thinking, Figures 3c and 3d illustrate that the presence of an illiquidity premium substantially increases the consumption potential. At the same time, it also exacerbates the overallocation problem. The widening grey areas

reflect the resulting increased variability in realized consumption rates as a response to the overallocation issue. In those cases, also the median allocation rate (indicated by the black dash on the curve) notably exceeds the SAA level (the diamond at the top of the curve). Overall, a higher (ξ^*), particularly driven by the high illiquidity premia or diversification potential in the private asset, also contributes to greater consumption reductions during periods of illiquidity.

Figure 3: Consumption Rates with Private Asset (10-year illiquidity)

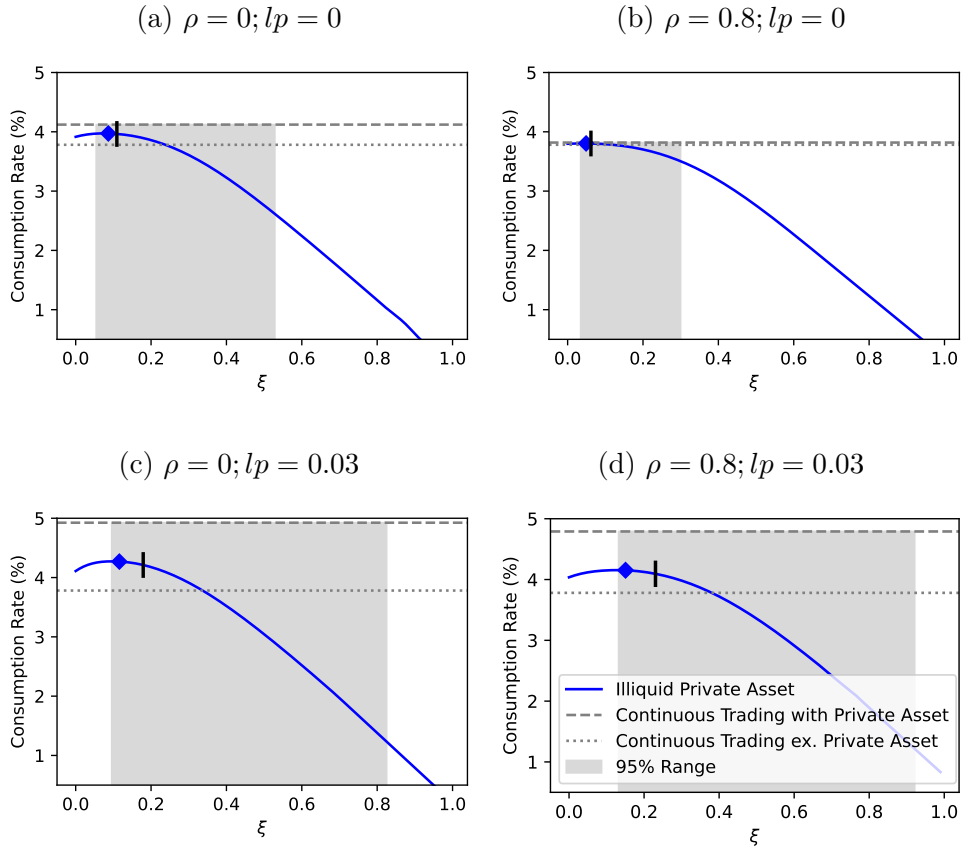

Note. This set of figures illustrate the effects of private asset illiquidity on consumption rates. The solid blue curve represents the consumption rate of an investor holding a private asset with a 10-year average illiquidity; the upper dashed line shows the consumption rates assuming full liquidity of the private asset; and the lower dashed lines show the rate when investment is made in liquid public assets solely. The shaded gray areas denote the 95% range of realized consumption rates, capturing the variability introduced by illiquidity constraints. Panels (a) and (c) assume that the private asset is uncorrelated with any publicly traded asset. Panels (c) and (d) assume a 3% illiquidity premium. The black arrow marks the median realized consumption rate, while the diamond indicates the consumption at the strategic allocation in the private asset.

Quantifying the benefits of optimal allocation to private assets: Next, we consider the benefits and costs of investing in an illiquid asset. For this purpose, we quantify investor welfare in risk-adjusted terms as the certainty equivalent consumption (CEC) associated with the optimal investment strategy (see Section 2.2). The CEC with illiquidity is a function of the initial allocation ξ_t, as derived in Equation (14). The solid blue curve in Figure 5 illustrates this. Given the dynamic principal of optimality embedded in the model, realizing this CEC is conditional on the investor optimally adjusting the portfolio tactical allocation and returning to the optimal strategic private asset allocation ξ^* given by the model at the next liquidity opportunity. The solid gray line shows this optimal strategic target. The vertical dashed gray line, on the other hand, is the Merton optimal allocation, i.e. assuming that continuous rebalancing opportunities exist for the private asset.

Define the allocation benefit from investing in the private asset class as the improvement in CEC relative to investing only in liquid public assets. Formally:

$$\text{Allocation Benefit} = \frac{CEC(\xi^*)}{CEC_m(\xi = 0)} - 1, \tag{15}$$

where $CEC(\xi^*)$ represents the certainty equivalent consumption with the illiquid asset at its optimal strategic weight, and $CEC_m(\xi = 0)$ corresponds to the CEC when the private asset is excluded from the investment universe altogether, with the optimal policies evaluated through a Merton model.

Figure 4 summarizes the size of this allocation benefits. First, with no liquidity premia (Chart 4a), the allocation benefit is relatively large initially (around 10%) when the private asset is diversifying and highly liquid, but declines gradually when the diversification potential of the asset cannot be fully realized with higher illiquidity. When the asset is not diversifying, the allocation benefit remains minimal, starting at around 1.5% and declining to zero. Factoring in a liquidity premium for the private asset, the benefit

declines from 30% to around 10% at the high end of the illiquidity parameter.

Figure 4: Allocation Benefit with Private Asset

(a) No Illiquidity Premium (b) With Illiquidity Premium

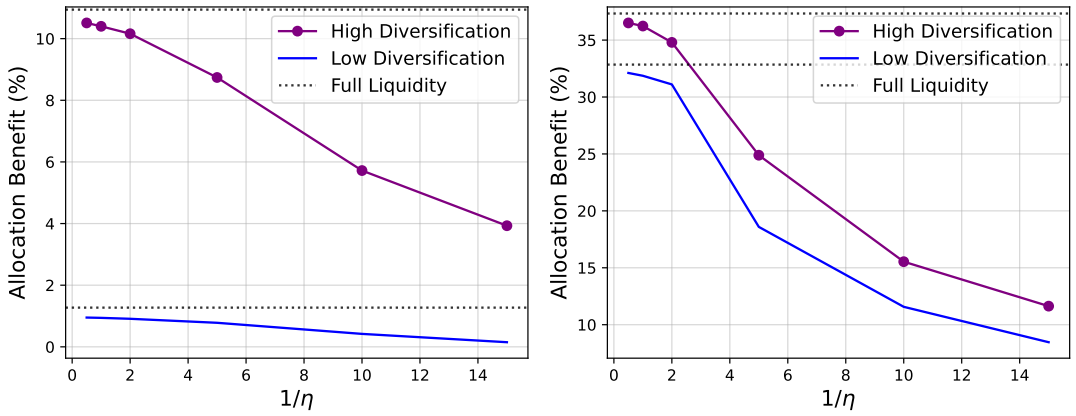

Note. This figure quantifies the benefit of allocating to the illiquid asset. The benefit is measured as the percentage increase in certainty equivalent consumption. Figure (a) shows the benefit when no illiquidity premia exists. Figure (b) specifies 3% illiquidity premia. The dotted lines correspond to the benefit evaluated with a fully liquid asset through the Merton model.

Misallocation risk with private assets: Finally, define the misallocation loss as the potential welfare loss from ignoring the illiquidity risk of the private asset. Using the Merton model and assuming erroneously that the private asset allocation is adjustable continuously leads to over-optimistic allocation recommendations, which later on will constrain investment consumption. Formally, we define:

$$\text{Misallocation Risk} = -\left(\frac{CEC(\xi^{liquid})}{CEC(\xi^{*})} - 1\right), \tag{16}$$

where $CEC(\xi^{liquid})$ is the CEC in the model with illiquidity at the Merton optimal allocation to private assets, and the $CEC(\xi^{*})$ is evaluated at the optimal allocation with illiquidity properly considered. Note that this formulation of the misallocation risk represents a lower bound on the actual loss. The $CEC(\xi)$ function implicitly assumes that even when the private asset is misallocated the rest of the portfolio and the consumption

Figure 5: Investor Welfare with Private Asset (10-year illiquidity)

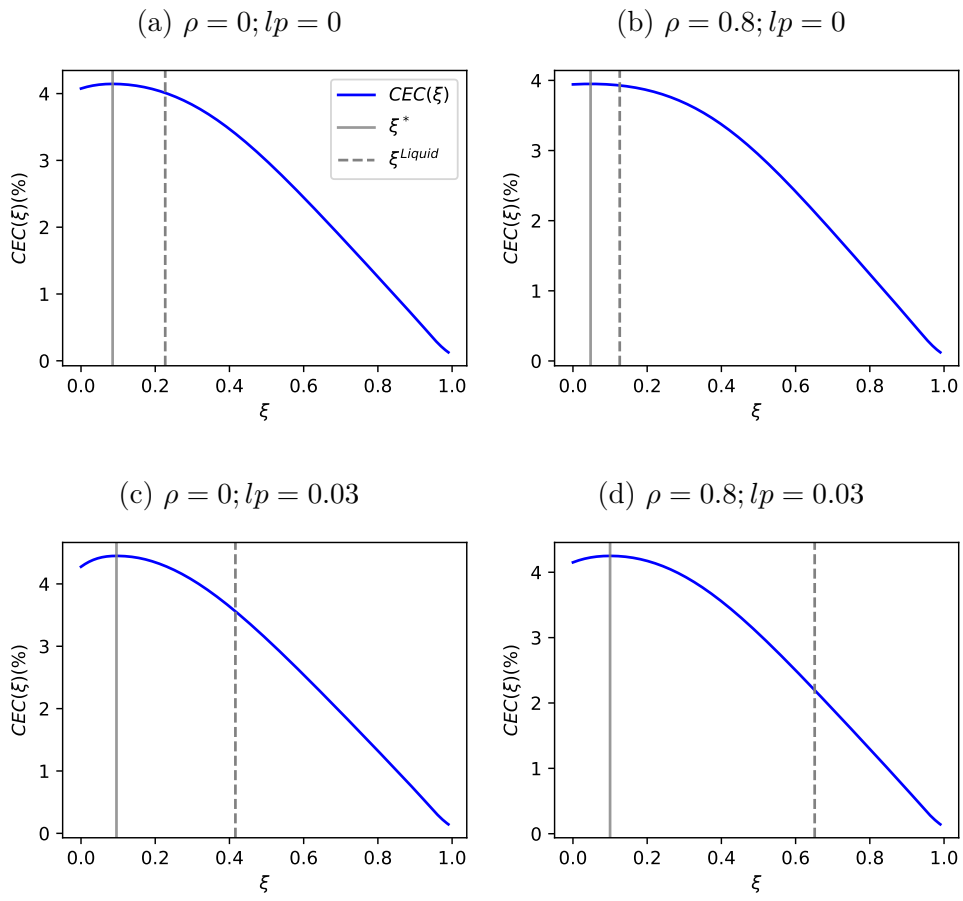

Note. This set of figures illustrates the effects of private asset illiquidity on investor welfare, measured as the Certainty Equivalent Consumption rate as a percent of total wealth. The solid blue curve represents the CEC of an investor holding a private asset with a 10-year average non-trading time as a function of the initial allocation to the private asset, ξ. The dashed vertical lines indicate optimal allocation ignoring liquidity risk. Panels (a) and (c) assume that the private asset is uncorrelated with any publicly traded asset and bears no illiquidity premium. Panels (c) and (d) assume a 3% illiquidity premium.

rate remain optimized.

Judging by the gap between the solid and the dashed vertical lines in Figure 5, indicating the optimal allocation to the illiquid asset with illiquidity risk (the model in this paper) and without illiquidity risk (the Merton model) respectively, the misallocation risk increases with the convexity of the CEC curve and with the properties of the private illiquid asset. When the expected waiting time to rebalance the portfolio is high, or when correlations between the private asset and the liquid assets are lower, the CEC curve becomes more convex. Also, a positive illiquidity premium and low correlation provide over-optimistic Merton allocations, exacerbating the misallocation loss.

4 Strategic Allocation with Private Asset Classes

4.1 Model Calibration

SAA decisions are inherently forward-looking, making the direct use of historical returns subject to parametrization risk with obsolete data. Using CMAs that merge insights from quantitative researchers, industry experts, and academics is a standard way among institutional investors to overcome this historical bias when preparing their strategic allocation (Terhaar et al., 2003; Andonov and Rauh, 2022; Couts et al., 2023). Following this approach, now I part from the stylized calibration of the previous section and evaluate the model using long-term asset class expectations (CMAs) compiled by third-party analysts. In particular, I use the CMAs compiled by JP Morgan as of 2025. JP Morgan produce their CMAs using a combination of quantitative and qualitative inputs and provide a forward-looking 10-15 year outlook on returns, volatilities, and correlations across various publicly and privately traded asset classes.[5] Their CMAs are publicly available,

[5]Further details on the approaches used by JP Morgan are available in their methodological guide: https://am.jpmorgan.com/content/dam/jpm-am-aem/global/en/insights/portfolio-insights/ltcma/noindex/ltcma-methodology-handbook.pdf

and Table (4) summarizes the input data for the asset classes used in this study.[6]

Using CMAs instead of historical data also avoids other biases inherent in the historical returns of private assets, for which infrequent trading tends to over-smooth historical returns, leading to downward-biased estimates of asset variances and correlations; secondary markets are often thin, with data frequently derived from appraisals; private equity managers often have discretion over the timing of valuation reporting, creating incentives to disclose performance only when it is favorable; and even when trading occurs, observable market values are more likely to emerge when asset prices are high and sellers are active.[7] In addition, the private equity expected returns in CMAs are net of the fees and expenses charged by managers, so they reflect the final returns to the investor, and thus are on the same level playing field as the traditional asset classes.

In the model, the liquid investment universe is mapped to the traditional asset classes in public equity (including small and large caps, and international stocks) and fixed income (including long-term treasury bonds and corporates). The risk-free asset, calibrated to the expected return on the money market rate, is classified under short-term fixed income. I focus on a long-only investor and examine five distinct cases, in each of which, I add to the investment universe only one private asset class at a time: Core Real Estate, Infrastructure, Private Equity, Diversified Hedge Funds, or Macro Hedge Funds. This approach mirrors an investor interested in exploring a single private asset class out of several alternatives. From a modeling perspective, this also simplifies the analysis by avoiding the complexities of establishing dependencies between the arrivals of liquidity events (multiple Poisson processes) across several illiquid asset classes.

The expected waiting times associated with the illiquid private assets, on the other hand, are calibrated based on estimates from the academic literature. I rely on crude

[6]See https://am.jpmorgan.com/content/dam/jpm-am-aem/global/en/insights/portfolio-insights/ltcma/noindex/ltcma-full-report.pdf

[7]For a summary of this evidence, see Ang (2014); Brown et al. (2023, 2019).

Table 4: Asset Class Characteristics and Correlation Matrix

Asset Class			Return	Volatility	Sharpe	Correlation									
						1	2	3	4	5	6	7	8	9	10
Fixed Income	Money Market*	0	3.1	-	-										
	U.S. Long Treasuries	1	4.3	12.83	0.09										
	U.S. Long Corporate Bonds	2	4.9	12.08	0.15	0.67									
Equity	U.S. Large Cap	3	6.7	16.26	0.22	-0.03	0.47								
	U.S. Small Cap	4	6.9	20.73	0.18	-0.1	0.38	0.9							
	EAFE Equity	5	8.1	17.61	0.28	-0.04	0.52	0.88	0.8						
Liquid Alternatives	U.S. REITs	6	8	17.22	0.28	0.19	0.54	0.77	0.76	0.71					
Private Assets	U.S. Core Real Estate	7	8.1	11.32	0.44	-0.19	-0.02	0.35	0.29	0.27	0.46				
	Global Core Infrastructure	8	6.3	11.01	0.29	0.24	0.2	0.47	0.41	0.55	0.36	0.32			
	Private Equity	9	9.9	19.62	0.35	-0.37	0.26	0.78	0.75	0.8	0.53	0.34	0.62		
	Diversified Hedge Funds	10	4.9	5.80	0.31	-0.21	0.31	0.68	0.64	0.7	0.42	0.32	0.43	0.79	
	Macro Hedge Funds	11	3.8	7.00	0.1	-0.09	0.05	0.16	0.14	0.24	0.1	0.01	0	0.26	0.48

Note. This table shows the Capital Market Assumptions based on the JP Morgan's report for 2025. These include the expected (net) returns, standard deviations of the asset classes considered here, and the correlations between them.

approximations for the average expected time to redeem the investment in each asset class. The timing of exit or redemption for the private asset classes considered here is uncertain, justifying the Poisson assumption of the liquidity arrivals. Secondary markets for private equity and hedge funds remain nascent, characterized by thin trading volumes and significant pricing discounts (Kleymenova et al., 2012; Ramadorai, 2012; Nadauld et al., 2019). For this reason, I do not explicitly model an exit option from the illiquid private investment through the secondary market.

For private equity, Metrick and Yasuda (2010) report a median exit time of approximately five years, but it can extend to more than 10 years. Andonov et al. (2021) observe comparable exit times for infrastructure investments, as most investors access these assets through closed-end funds structured similarly to private equity. Bitsch et al. (2010) further highlight that while the underlying assets of infrastructure funds often have long lifespans, the funds themselves exhibit exit times similar to those of private equity funds. Based on these findings, I adopt a calibration for the illiquidity parameter η of 1/5 and 1/10 for private equity and infrastructure funds. With the rise of direct investments (typically in the form of co-investments, see Fang et al. (2015)), it is worthwhile exploring also more illiquid investments with $\eta = 1/10$. For Real Estate funds, Fisher and Hartzell (2016) report median exit times ranging from 4.25 to 5.5 years, supporting again

a calibration of $\eta = 1/5$.

Hedge funds, in contrast, have much shorter illiquidity horizons related to gates imposed by the manager or varying lock-up periods and redemption notice requirements. Although these contractual clauses are typically known once a fund manager is selected, ex-ante they vary across funds in the asset class. I calibrate their illiquidity to $\eta = 1$, aligning with the findings reported in Schaub and Schmid (2013).

4.2 Empirical Results

Table 5: Strategic Asset Allocation and Welfare under Illiquidity Scenarios

	Private Equity			Infrastructure			Real Estate		Diversified Hedge Funds		Macro Hedge Funds	
	Liquid	Illiquid 5Y	Illiquid 10Y	Liquid	Illiquid 5Y	Illiquid 10Y	Liquid	Illiquid	Liquid	Illiquid	Liquid	Illiquid
Fixed Income	63.20	67.02	67.99	49.21	56.78	62.94	30.57	54.87	23.07	29.13	57.97	58.25
- Short Term	30.92	48.56	53.81	47.11	51.74	55.55	9.13	39.89	8.99	15.71	47.90	48.18
- Long Term	32.27	18.47	14.18	2.10	5.03	7.39	21.44	14.99	14.08	13.41	10.07	10.07
Equity	0.19	4.66	11.17	5.20	10.17	14.13	18.02	20.43	3.34	5.29	16.47	16.50
Liquid Alternatives	0.40	11.14	11.93	16.39	14.95	13.83	0.05	4.07	14.42	14.08	13.34	13.33
Private Assets	36.15	17.09	8.82	29.12	18.03	9.01	51.31	20.55	59.13	51.46	12.13	11.84
CEC	4.59	4.31	4.14	4.13	4.09	4.02	5.25	4.60	4.24	4.21	3.95	3.95
Median Realized ξ	36.15	20.34	13.41	29.12	20.44	12.13	51.31	24.60	59.13	51.46	12.13	11.84
Median Realized c	4.32	4.09	3.94	3.95	3.92	3.86	4.83	4.31	3.98	4.02	3.81	3.81
Allocation Benefit	16.65	9.51	5.11	4.78	3.87	2.20	33.46	16.78	7.70	6.98	0.27	0.27
Misallocation Risk	-	3.69	12.49	-	0.58	5.43	-	16.68	-	0.19	-	0.00

Note. This table shows the optimal strategic asset allocations for a variety of illiquid asset classes in the case of a long-only investor.

Table 5 presents the model solution for the optimal strategic allocation. Embedding illiquidity into the portfolio optimization influences the investors' consumption rate, allocation decisions, and consequently their welfare, measured through the CEC. In each case, I first consider the hypothetical situation in which the private asset can be traded continuously. Comparing against this, one can see that the illiquidity risk of the private assets significantly alters the asset allocation of the portfolio. First, the allocation to the liquid asset classes is affected. The most notable shift is the substantial increase in short-term fixed-income allocations, due to, as noted earlier, the higher cash buffers needed to mitigate the risk of significant disruptions in consumption brought about by illiquidity. Note that the allocation to the risk-free asset (here: short-term fixed income) is high to start with, partially driven by the relatively high interest rate in the CMAs, and the fact

that there are no weight constraints on cash.

Second, the allocation to the private asset class is significantly reduced, particularly for private equity, where the allocation declines from 36.15% when illiquidity is ignored, to 17.09% for a five-year expected waiting time and further to 8.82% for a ten-year waiting time. This is accompanied by a substitution effect where the allocations to Public Equity and Liquid Alternatives (e.g., REITs) are increased, rising from zero to approximately 11.17% and 11.93%, respectively, in response to the reduced role of private equity. Similar reallocation patterns are observed for Real Estate, which is partially substituted by REITs; and Infrastructure, which is partially substituted by Public Equity. Hedge Funds, on the other hand, are comparatively much more liquid. Even though they show a similar trend, it is much more subdued. Among hedge fund strategies, Diversified Hedge Funds exhibit a more pronounced substitution effect due to their higher correlation with public equity, while Macro Hedge Funds maintain relatively stable allocations.

The inclusion of a private asset class in the portfolio, even after accounting for its illiquidity, yields measurable allocation benefits. These benefits, expressed as percentage increases in certainty equivalent consumption (CEC), range from 0.2% to 16%. The baseline CEC for a portfolio excluding private assets altogether is \$3.937 per \$100 invested, serving as a benchmark against which the allocation benefits are measured. The highest allocation benefit is observed for Real Estate, which provides high diversification advantages (judging by the low correlations with the rest of the investment universe in Table 4), while the lowest benefit is for Macro Hedge Funds due to their low risk-adjusted returns in the CMAs (Sharpe Ratio in Table 4). Considering illiquidity risk in the optimization, however, significantly lowers the estimated allocation benefit for almost all asset classes. The shift is most notable for Private Equity, where the allocation benefit drops from 16% when only variance risk is considered, down to 5% when the expected time between liquidity events is extended up to 10 years.

In addition, ignoring illiquidity produces higher allocations to the private asset classes, exposing investors to substantial welfare losses due to the misallocation, measured by (16). Allocating according to a liquid model leads to a 3% welfare loss for private equity assuming a five-year expected waiting time, and extends up to 12% for a ten-year waiting time. Infrastructure investments exhibit relatively low misallocation risks for 5-year expected waiting time but face up to a 5% welfare loss if the expected waiting time is extended to 10 years. Real Estate incurs the highest misallocation risk among private assets. As illustrated in Section 3, high diversification potential, on the flip side, is associated with lower possibility to hedge or substitute the illiquid asset, thus leading to higher potential misallocation loss under illiquidity. Even with a five-year waiting time, welfare losses due to misallocation can reach 16%. Hedge funds demonstrate significantly lower misallocation risks.

5 Conclusion

This paper underscored the role of illiquidity when private asset classes are part of the investor's strategic allocation mix, and quantifies the degree to which they improve the certainty equivalent consumption of a long-term investor. I find that the allocation gains are tempered when illiquidity risk is properly accounted for. Ignoring it, on the other hand, can lead to overallocation and significant welfare losses, particularly for highly illiquid assets such as private equity and real estate.

The dynamic portfolio choice model presented here provides a unified framework to handle illiquid private assets. Further extensions can capture the nuances of each specific private asset class. In addition, fixed costs of investment, typically a concern for smaller investors, can be included in the framework as private assets require strong expertise and a due diligence process which comes at an initial cost to develop. Also, as secondary

markets become more liquid and a more viable exit option, including them in the model may become more relevant. Yet, the dynamic portfolio choice model presented here provides an intuitive framework for the discussion of illiquidity in the asset allocation problem, and allows the use of CMAs typically part of the institutional investor's asset allocation toolbox.

References

Andonov, A. and Rauh, J. D. 2022. The return expectations of public pension funds. *The Review of Financial Studies*, 35(8):3777–3822.

Andonov, A., Eichholtz, P., and Kok, N. 2015. Intermediated investment management in private markets: Evidence from pension fund investments in real estate. *Journal of Financial Markets*, 22:73–103.

Andonov, A., Kräussl, R., and Rauh, J. 2021. Institutional investors and infrastructure investing. *The Review of Financial Studies*, 34(8):3880–3934.

Andonov, A., Bonetti, M., and Stefanescu, I. 2023. Choosing pension fund investment consultants. *Available at SSRN 4306217*.

Ang, A. 2014, *Asset Management*. Oxford University Press.

Ang, A. and Sorensen, M. 2012. Risks, returns, and optimal holdings of private equity: A survey of existing approaches. *The Quarterly Journal of Finance*, 2(03):1250011.

Ang, A., Papanikolaou, D., and Westerfield, M. M. 2014. Portfolio choice with illiquid assets. *Management Science*, 60(11):2737–2761.

Ang, A., Chen, B., Goetzmann, W. N., and Phalippou, L. 2018. Estimating private equity returns from limited partner cash flows. *The Journal of Finance*, 73(4):1751–1783.

Begenau, J., Liang, P., and Siriwardane, E. 2025. The rise of alternatives. *Working Paper*.

Bitsch, F., Buchner, A., and Kaserer, C. 2010. Risk, return and cash flow characteristics of infrastructure fund investments. *EIB papers*, 15(1):106–136.

Bollen, N. P. and Sensoy, B. A. 2022. How much for a haircut? illiquidity, secondary markets, and the value of private equity. *Financial Management*, 51(2):501–538.

Boyle, P. P. and Lin, X. 1997. Optimal portfolio selection with transaction costs. *North American Actuarial Journal*, 1(2):27–39.

Brennan, M. J., Schwartz, E. S., and Lagnado, R. 1997. Strategic asset allocation. *Journal of Economic Dynamics and Control*, 21(8-9):1377–1403.

Broeders, D. W., Jansen, K. A., and Werker, B. J. 2021. Pension fund's illiquid assets allocation under liquidity and capital requirements. *Journal of pension economics & finance*, 20(1):102–124.

Brown, G. W., Gredil, O. R., and Kaplan, S. N. 2019. Do private equity funds manipulate reported returns? *Journal of Financial Economics*, 132(2):267–297.

Brown, G. W., Ghysels, E., and Gredil, O. R. 2023. Nowcasting net asset values: The case of private equity. *The Review of Financial Studies*, 36(3):945–986.

Cai, Y., Judd, K. L., and Xu, R. 2013. Numerical Solution of Dynamic Portfolio Optimization with Transaction Costs. *NBER Working Paper No. w18709*.

Campbell, J. Y., Chacko, G., Rodriguez, J., and Viceira, L. M. 2004. Strategic asset allocation in a continuous-time VAR model. *Journal of Economic Dynamics and Control*, 28(11):2195–2214.

Chen, H., Gambarotta, G., Scheidegger, S., and Xu, Y. 2025. A dynamic model of private asset allocation. *arXiv preprint arXiv:2503.01099*.

Cochrane, J. H. 2022. Portfolios for long-term investors. *Review of Finance*, 26(1):1–42.

Couts, S. J., Gonçalves, A. S., and Loudis, J. 2023. The subjective risk and return expectations of institutional investors. *Fisher College of Business Working Paper*, 14.

Dai, M., Jin, H., and Liu, H. 2011. Illiquidity, position limits, and optimal investment for mutual funds. *Journal of Economic Theory*, 146(4):1598–1630. ISSN 0022-0531.

Dimmock, S. G., Wang, N., and Yang, J. 2023. The endowment model and modern portfolio theory. *Management Science*, 70(3):1554–1579.

Fang, L., Ivashina, V., and Lerner, J. 2015. The disintermediation of financial markets: Direct investing in private equity. *Journal of Financial Economics*, 116(1):160–178.

Fisher, L. M. and Hartzell, D. J. 2016. Class differences in real estate private equity fund performance. *The Journal of Real Estate Finance and Economics*, 52:327–346.

Franzoni, F., Nowak, E., and Phalippou, L. 2012. Private equity performance and liquidity risk. *Journal of Finance*, 67(6):2341–2373.

Gennotte, G. and Jung, A. 1994. Investment Strategies under Transaction Costs: The Finite Horizon Case. *Management Science*, 40(3):385–404.

Giesecke, O. and Rauh, J. 2023. Trends in state and local pension funds. *Annual Review of Financial Economics*, 15:221–238.

Giommetti, N. and Sorensen, M. 2021. Optimal allocation to private equity. *Tuck School of Business Working Paper*, (3761243).

Gourier, E., Phalippou, L., and Westerfield, M. M. 2024. Capital commitment. *The Journal of Finance*, 79(5):3407–3457.

Gredil, O., Liu, Y., and Sensoy, B. A. 2020. Diversifying private equity. *Available at SSRN 3535677*.

Ilmanen, A., Chandra, S., and McQuinn, N. 2020. Demystifying illiquid assets: Expected returns for private equity. *The Journal of Alternative Investments*, 22(3):8–22.

Jansen, K. A. and Werker, B. J. 2022. The shadow costs of illiquidity. *Journal of Financial and Quantitative Analysis*, 57(7):2693–2723.

Judd, K. L. 1998, *Numerical Methods in Economics*. MIT Press.

Kim, J. H., Lee, Y., Kim, W. C., and Fabozzi, F. J. 2021. Mean–variance optimization for asset allocation. *The Journal of Portfolio Management*, 47(5):24–40.

Kleymenova, A., Talmor, E., and Vasvari, F. P. 2012. Liquidity in the secondaries private equity market. *Working paper, London Business School*.

Longstaff, F. A. 2001. Optimal Portfolio Choice and the Valuation of Illiquid Securities. *Review of Financial Studies*, 14(2):407–31.

Luxenberg, E., Boyd, S., van Beek, M., Cao, W., and Kochenderfer, M. Strategic asset allocation with illiquid alternatives. In *Proceedings of the third ACM international conference on AI in finance*, pages 249–256, 2022.

Magill, M. J. P. and Constantinides, G. M. 1976. Portfolio selection with transactions costs. *Journal of Economic Theory*, 13(2):245–263.

Martellini, L. and Milhau, V. 2020. Does factor investing improve investor welfare? A multi-asset perspective. *Journal of Portfolio Management*, 46(6):32–53.

Metrick, A. and Yasuda, A. 2010. The economics of private equity funds. *The Review of Financial Studies*, 23(6):2303–2341.

Miklós, K. and Ádám, S. 2002. Portfolio Choice with Illiquid Assets. Rajk László

Szakkollégium Working Papers 6, Rajk László College.

Nadauld, T. D., Sensoy, B. A., Vorkink, K., and Weisbach, M. S. 2019. The liquidity cost of private equity investments: Evidence from secondary market transactions. *Journal of Financial Economics*, 132(3):158–181.

Ramadorai, T. 2012. The secondary market for hedge funds and the closed hedge fund premium. *Journal of Finance*, 67(2):479–512.

Rust, J. 1996. Numerical dynamic programming in economics. *Handbook of computational economics*, 1:619–729.

Schaub, N. and Schmid, M. 2013. Hedge fund liquidity and performance: Evidence from the financial crisis. *Journal of Banking & Finance*, 37(3):671–692.

Sefiloglu, O. 2022. In pursuit of information: Information asymmetry in private equity commitments. *Available at SSRN 4239801*.

Terhaar, K., Staub, R., and Singer, B. D. 2003. Appropriate policy allocation for alternative investments. *The Journal of Portfolio Management*, 29(3):101–110.

Van Binsbergen, J. H., Brandt, M. W., and Koijen, R. S. 2008. Optimal decentralized investment management. *The Journal of Finance*, 63(4):1849–1895.

Zabel, E. 1973. Consumer Choice, Portfolio Decisions, and Transaction Costs. *Econometrica*, 41(2):321–35.

Annex:

A Discretization & Numerical Solution Methods

This section outlines the numerical approaches used to find the reduced-form value function $H(\xi)$ and the optimal controls for the portfolio choice problem with illiquidity defined in Section 2.[8]

A.1 The trading probability and the Poisson process

Figure 6: Relationship between p and η

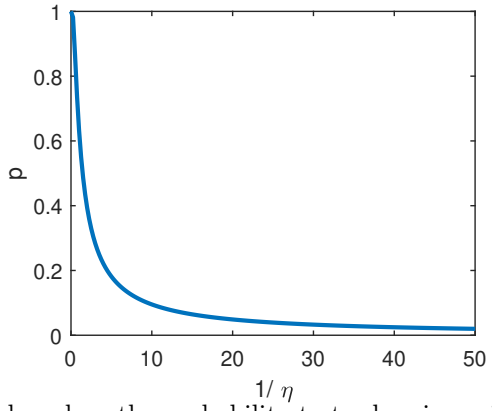

The plot shows the connection based on the probability to trade p in an illiquid asset within a year and $1/\eta$, the average waiting time in years between trades.

First, we define the probability p with which the investor trades the illiquid asset over a discrete time period Δt. This probability will be a function of the intensity η of the Poisson process that indicates the relocation opportunities. To show that formally, note that a Poisson process has stationary and independent increments, where the number of events that occur during any time increment of length Δt is Poisson distributed with mean $\eta\Delta t$. Then the probability that n events occur over the time increment can be written

[8]The model presented here and code to reproduce the results of this paper is available at https://github.com/danielkdimitrov/portfolioChoiceIlliq

as: $P(N_{t+\Delta t} - N_t = n) = \mathrm{e}^{-\eta\Delta t}\frac{(\eta\Delta t)^n}{n!}$. We can then show that p, as the probability of having at least one trading event over the time period Δt is such that

$$p = 1 - \mathrm{e}^{-\eta\Delta t} \tag{17}$$

Figure 6 illustrates this functional relationship over an annual horizon. It is well known that that $1/\eta$ represents the waiting time between two Poisson counts, so correspondingly, for a more appealing representation, I plot on the x-axis the expected time between two trades.

A.2 Discretizing the Bellamn equation:

Now, we look at time discretization of the dynamic optimization problem. The discretized Bellman equation can then be solved through value function iteration combined with standard numerical techniques.

Define the growth rate in liquid $R_{w,t+\Delta t}(c_t, \boldsymbol{\theta}_t) = \frac{W_{t+\Delta t}}{W_t}$ and illiquid wealth $R_{x,t+\Delta t} = \frac{X_{t+\Delta t}}{X_t}$ for the cases when rebalancing is not possible (i.e. $dI_t = 0$ in (5)), such that the Euler discretization of the continuous stochastic process (3) holds, ass:

$$\begin{aligned} R_{w,t+\Delta t} &= 1 + (r + \boldsymbol{\theta}_t'(\boldsymbol{\mu}_w - r\mathbb{1}) - c_t)\Delta t + \boldsymbol{\theta}_t'\boldsymbol{\sigma}_w\sqrt{\Delta t}\boldsymbol{\Delta Z}_t \\ R_{x,t+\Delta t} &= 1 + \mu_x\Delta t + \boldsymbol{\sigma}_x\sqrt{\Delta t}\boldsymbol{\Delta Z}_t \end{aligned} \tag{18}$$

where $\boldsymbol{\Delta Z}_t$ is a column vector of standard normal random variables.[9]

Then, we can define the growth in total wealth $R_{q,t+\Delta t} = \frac{Q_{t+\Delta t}}{Q_t}$, and the change in

[9] A Gaussian quadrature approach will be used for the space-discretization of the normal distribution and for the evaluation of the expectations in the Euler equation presented next (cf. Section A.4).

the illiquid asset share $\xi_{t+\Delta t}$ as:

$$\begin{aligned} R_{q,t+\Delta t} &= (1-\xi_t)R_{w,t+\Delta t} + \xi R_{x,t+\Delta t} \\ \xi_{t+\Delta t} &= \xi_t \frac{R_{x,t+\Delta t}}{R_{q,t+\Delta t}} \end{aligned} \tag{19}$$

Proposition: The dynamic problem defined in Section 2 can be solved through the discterized Bellman equation of the form:

$$\begin{aligned} &H(\xi_t) = \\ &\max_{(\theta_t, c_t)} \left\{ u(c_t(1-\xi_t))\Delta t + \delta \left(pH^* E_{\xi_t}\left[R_{q,t+\Delta t}^{1-\gamma}\right] + (1-p)E_{\xi_t}\left[R_{q,t+\Delta t}^{1-\gamma} H(\xi_{t+\Delta t})\right]\right)\right\} \end{aligned} \tag{20}$$

where p is the discretized probability of being able to trade next period (cf. Equation (17)), $\delta = \mathrm{e}^{-\beta \Delta t}$ is a discount factor, $H(.)$ is the reduced value function of Equation (8), and $H^* = \max_\xi H(\xi)$.

Proof: It is easy to derive equations (19):

$$\begin{aligned} R_{q,t+\Delta t} &= \frac{Q_{t+\Delta t}}{Q_t} = \frac{W_t R_{w,t+\Delta t} + X_t R_{x,t+\Delta t}}{Q_t} \\ &= (1-\xi_t)R_{w,t+\Delta t} + \xi R_{x,t+\Delta t} \\ \xi_{t+\Delta t} &= \frac{X_{t+\Delta t}}{Q_{t+1}} = \frac{X_t}{Q_t}\frac{X_{t+\Delta t}}{X_t}\frac{Q_t}{Q_{t+\Delta t}} \\ &= \xi_t \frac{R_{x,t+\Delta t}}{R_{q,t+\Delta t}} \end{aligned}$$

The dynamic optimization problem with illiquid assets is defined through the intertemporal objective given in ((6)) and the law of motion given in (5). Using the Bellman principle of optimality we can tranform the dynamic problem into its discret time version[10]:

$$V(W_t, X_t) = \max_{(\theta_t, dI_t, c_t \in \mathcal{A})} \{u(C_t)\Delta t + \delta E_{W_t, X_t}[V(W_{t+\Delta t}, X_{t+\Delta t})]\}$$

with $\delta = \mathrm{e}^{-\beta \Delta t}$ as a discrete-time discount factor, and where the expectation is conditional on the initial liquid wealth W_t and illiquid wealth X_t at time t. Using the homothetic properties of the CRRA utility from Equation 8, we can rewrite the Bellman equatoin:

$$V(Q_t, \xi_t) = \max_{(\theta_t, \xi_t, c_t \in \mathcal{R})} \{u(c_t(1-\xi_t)Q_t)\Delta t + \delta E_{Q_t,\xi_t}[V(Q_{t+\Delta t}, \xi_{t+\Delta t})]\}$$
$$Q_t^{(1-\gamma)} H(\xi_t) = \max_{(\theta_t, \xi_t, c_t \in \mathcal{R})} \{Q_t^{(1-\gamma)} u(c_t(1-\xi_t))\Delta t + \delta E_{Q_t,\xi_t}[Q_{t+\Delta t}^{(1-\gamma)} H(\xi_{t+\Delta t})]\}$$

The investor will set $\xi_{t+\Delta t} = \xi^*$ whenever trading is possible, coming to the top of the value function, $H(\xi)$. If trading is not possible, the investor cannot rebalance and is stuck with suboptimal levels of illiquid holdings $\xi_{t+\Delta t}$, and the ratio will float away in a random direction from last period's value as the prices of the two risky assets move. Since that case is suboptimal, the value function will be lower and at $H(\xi_{t+\Delta t})$. This is illustrated in Figure 7.

Combining the two, we can write the Bellman equation as:

$$Q_t^{(1-\gamma)} H(\xi_t) =$$
$$\max_{(\theta_t, dI_t, c_t \in \mathcal{R})} \left\{ Q_t^{(1-\gamma)} u(c_t(1-\xi_t))\Delta t + \delta \Big(p E_{Q_t}[Q_{t+\Delta t}^{(1-\gamma)}] H^* + (1-p) E_{Q_t}[Q_{t+\Delta t}^{(1-\gamma)} H(\xi_{t+\Delta t})] \Big) \right\}$$

Note, that by canceling out Q_t and by embedding it in the expectations the conditional part of the expectation with respect to Q can be dropped and we arrive to Equation (20). □

[10]To get intuition on the discretization step from the classic Merton case, note that the discrete Bellman equation $V(W_t) = \sup_{(\pi_t, C_t)} \{u(C_t)\Delta t + \mathrm{e}^{-\beta \Delta t} E[V(W_{t+\Delta t})]\}$ can be shown to converge to its continuous counterpart for $\Delta t \to 0$. Multiply the equation by $\mathrm{e}^{\beta \Delta t}$, subtract $V(W)$ from both sides and divide by Δt and this results in: $\frac{\mathrm{e}^{\beta \Delta t} - 1}{\Delta t} V(W) = \sup_{(\pi_t \in \mathcal{R}^d, c_t \geq 0)} \{u(c_t) + \frac{1}{\Delta t} E_t[V(W_{t+\Delta t}) - V(W_t)]\}$

Let $\Delta t \to 0$, then $\mathrm{e}^{\beta \Delta t} \to 1$ and also by the L'Hôpital rule we have that $\frac{\mathrm{e}^{\beta \Delta t} - 1}{\Delta t} \to \beta$. As a result $\frac{1}{\Delta t} E_t[V(W_{t+\Delta t}) - V(W_t)] \to E_t[dV]$ which makes discretized equation equivalent to the continuous time version: $\sup_{(\boldsymbol{\pi}_t, C_t)} \mathrm{e}^{-\beta t} u(C_t) + E\left[d(\mathrm{e}^{-\beta t} V(W_t))\right] dt = 0$

Figure 7: Dynamic Asset Allocation and State Transition

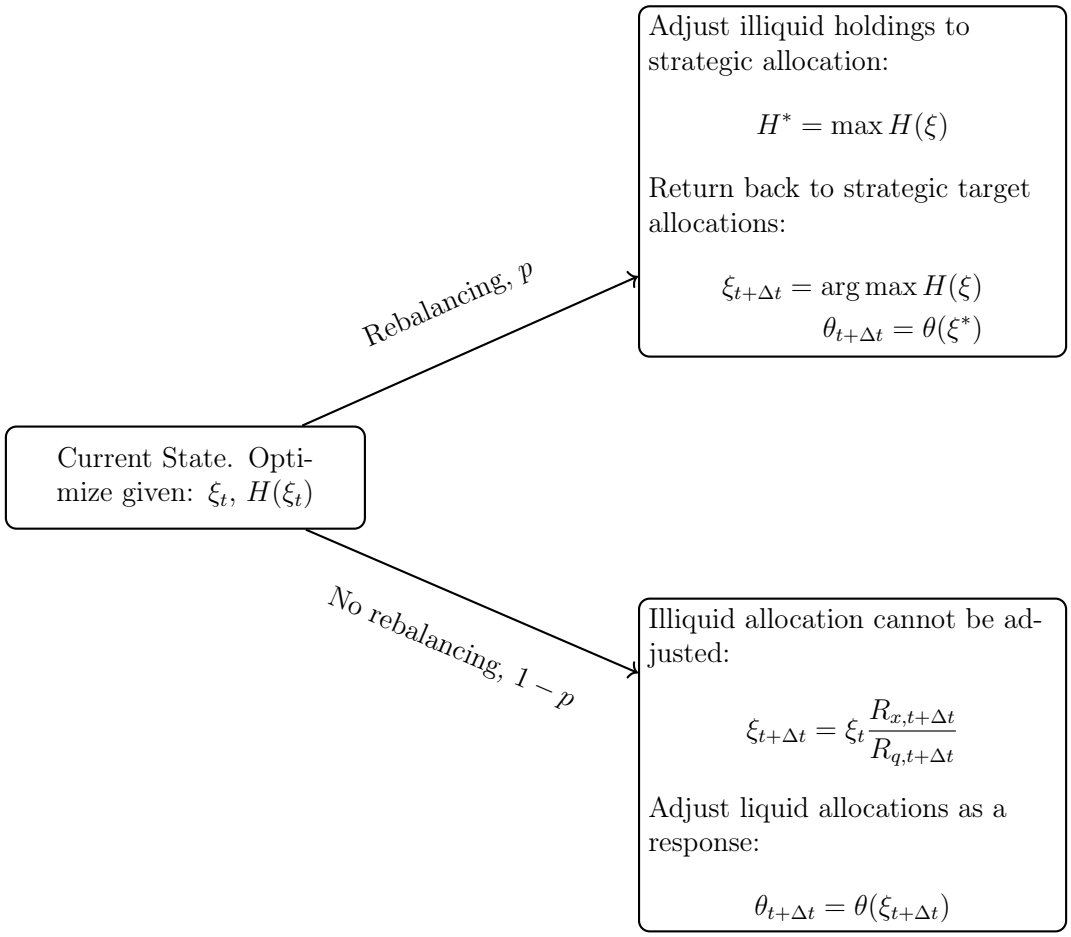

This chart illustrates the dynamics behind the optimal choice problem. In the coming period, the illiquid asset share floats freely to $\xi_{t+\Delta t}$. With probability p, the investor can trade in the illiquid asset and set it back to the optimal target of ξ^* by maximizing the known function $H(\xi)$. With probability $1-p$, the investor cannot trade and is stuck with the illiquid asset share of $\xi_{t+\Delta t}$.

A.3 Value Function Iteration:

Based on the discretization from Annex A.2, we can solve the portfolio choice dynamic problem through value function iteration. Discretizing ξ and evaluating the system one period ahead will allow us to iterate (20) until the iterative approximation of the value function $H(\xi)$ converges. The procedure will eventually yield a numerical approximation of the value function and the optimal solution for the policy functions $c(\xi)$ and $\theta(\xi)$. So, the goal is to find the approximating function $\tilde{H}(.)$ evaluated on a fixed grid $\tilde{\xi}$ which best

approximates the true theoretical function $H(\xi)$ underlying the HJB equation (C.2). We use the following iterative procedure:

Initialization: Discretize the random space (the random variables ΔZ_1 and ΔZ_2 in (18)) through a simulation or strategically selected (Gaussian) quadrature points (see Annex A.4).

Select an approximation grid of N gridpoints for ξ_t: $\tilde{\xi} = \{\xi_1, ..., \xi_N\} \in [0; 1)$, $j = 1, .., N$. I use $N = 20$. Select a class of approximating functions $\tilde{H}(\boldsymbol{a}; \tilde{\xi})$ which will approximate the true value function $H(\xi)$ and initialize the functional parameters $\boldsymbol{a}$. In particular I use a cubic spline due to its flexibility to capture strong curvature of the $H()$ function at the upper edge of ξ_t. Fitting the spline over the logarithmized values of the evaluated function also improves the convergences.

Select an initial guess for the maximum $\tilde{H}^*$ of the value function. As a starting point for the iteration we use the analytical two-asset Merton solution. We can then initiate the following iterative algorithm.

1. **Optimization:** For each ξ_j in the grid evaluate numerically optimal consumption and liquid asset allocation:

$$c^{*,k}, \theta^{*,k+1} = \arg\min \Big\{ u(c(1-\xi_j))\Delta t + \delta \Big(p\tilde{H}^* E\left[\hat{q}(c,\theta,\xi_j)^{1-\gamma}\right] + (1-p)E\left[\tilde{H}\left(\boldsymbol{a}^k; \hat{\xi}(c,\theta,\xi_j)\right)\hat{q}(c,\theta,\xi_j)^{1-\gamma}\right]\Big)\Big\}$$

   where $\hat{\xi}()$ and $\hat{q}()$ are next-period's dynamics calculated through (19), and $k = 1, ..., p$ is a counter measuring the iteration run.

2. **Update:** For each ξ_j and the optimal control policies found in the previous step update values of the value function that lie on the grid. Update the fit of the approximation function $\tilde{H}(\boldsymbol{a}^{k+1}; \xi)$ based on the new values. Update $\tilde{H}^{*,k+1} =$

$\arg\max_{\xi} \tilde{H}(\boldsymbol{a}^{k+1}; \xi)$.

3. **Stopping:** The algorithms stops if $\left\| \ln(-\tilde{H}(\boldsymbol{a}^{k+1}; \xi)) - \ln(-\tilde{H}(\boldsymbol{a}^{k}; \xi)) \right\|^2 < \epsilon$, otherwise we go to **Step 1**. I use $\epsilon = 0.1^6$

A.4 Gauss-Hermite Quadrature

I use quadrature approximation to evaluate the expectation terms in the numerical section of this paper. Multi-dimensional quadrature methods are less common, so I provide here a discussion of this approach, based on (Rust, 1996; Judd, 1998; Cai et al., 2013) and show how the recipe can be adapted to the discretized Bellman equation defined in (20).

Univariate case: We can start with a discussion of a one-dimensional quadrature. This will be used to generalize the problem to multiple dimensions. Gaussian quadrature approximates an integral of the form:

$$\int_a^b f(x)w(x)\,dx \approx \sum_{i=1}^{m} w_i f(x_i)$$

where $w(x)$ is a weight function, x_i are the quadrature nodes, w_i are the quadrature weights, and m is the number of quadrature points.

When dealing with integrals involving a normally distributed random variable (or the logarithm of a log-normally distributed variable), Gauss-Hermite (GH) quadrature is particularly useful. It applies a weight function $w(x) = e^{-x^2}$ and integrates over the entire real line. The nodes x_i are the roots of the Hermite polynomial, and the weights w_i are determined accordingly to accurately approximate the integral.

Note, however, that when evaluating the expectation of $f(y)$ for a random variable y

which is normally distributed with $y \sim N(\mu, \sigma)$ we have

$$\mathbb{E}(f(y)) = (2\pi\sigma^2)^{-1/2} \int_{-\infty}^{\infty} f(y) e^{-\frac{(y-\mu)^2}{2\sigma^2}} dy$$

To reconcile this with the GH approximation, we first use a change of variable $y = \sqrt{2}\sigma x + \mu$ and then apply the given quadrature approximation such that

$$\mathbb{E}(f(\sqrt{2}\sigma x + \mu)) = (\pi)^{-1/2} \int_{-\infty}^{\infty} f(\sqrt{2}\sigma x + \mu) e^{-x^2} dx \approx \frac{1}{\sqrt{\pi}} \sum_{i=1}^{m} w_i f(\sqrt{2}\sigma x_i + \mu)$$

Multivariate case: Similarly, for a multivariate normal vector $\boldsymbol{y} \sim N(\boldsymbol{\mu}, \boldsymbol{\Sigma})$, where $\boldsymbol{\mu}$ is an $n \times 1$ mean vector and $\boldsymbol{\Sigma}$ is a positive semi-definite covariance matrix, and $f(\boldsymbol{x}) : \mathbb{R}^n \to \mathbb{R}$ a scalar-valued function, the expectation $\mathbb{E}[f(\boldsymbol{y})]$ can be evaluated using a change of variable after performing a Cholesky decomposition $\boldsymbol{\Sigma} = \boldsymbol{\sigma}\boldsymbol{\sigma}^\top$. By substituting $\boldsymbol{y} = \sqrt{2}\boldsymbol{\sigma}\boldsymbol{x} + \boldsymbol{\mu}$, the integral

$$\mathbb{E}[f(\boldsymbol{Y})] = \frac{1}{(2\pi)^{N/2}|\boldsymbol{\Sigma}|^{1/2}} \int_{\mathbb{R}^N} f(\boldsymbol{y}) e^{-\frac{1}{2}(\boldsymbol{y}-\boldsymbol{\mu})^\top \boldsymbol{\Sigma}^{-1}(\boldsymbol{y}-\boldsymbol{\mu})} d\boldsymbol{y}$$

can be transformed to:

$$\mathbb{E}[f(\boldsymbol{Y})] = \frac{1}{\pi^{N/2}} \int_{\mathbb{R}^n} f(\sqrt{2}\boldsymbol{\sigma}\boldsymbol{x}_i + \boldsymbol{\mu}) e^{-\boldsymbol{x}^\top \boldsymbol{x}} d\boldsymbol{x}$$

where $\boldsymbol{x}_i$ is a $n \times 1$ vector quadrature node for $i = 1, \ldots, m$.

Then, in the multi-dimensional space, we can use the quadrature product rule to perform the approximation

$$\mathbb{E}[f(\boldsymbol{Y})] \approx \frac{1}{\pi^{n/2}} \sum_{i_1=1}^{m} \cdots \sum_{i_n=1}^{m} w_{i_1} \ldots w_{i_n} \cdot f\left(\sqrt{2}\boldsymbol{\sigma}\boldsymbol{x}_{i_1,i_2,\ldots,i_n} + \boldsymbol{\mu}\right) = \tag{21}$$

where $\boldsymbol{x}_{i_1,i_2,\ldots,i_n} = \begin{pmatrix} x_{i_1}, & x_{i_2}, & \ldots, & x_{i,n} \end{pmatrix}'$ is a vector representing the i-th multivariate quadrature node.[11] In particular, for further clarity we can write

$$f\left(\sqrt{2}\boldsymbol{\sigma}\boldsymbol{x}_{i_1,i_2,\ldots,i_n} + \boldsymbol{\mu}\right) \equiv f\begin{pmatrix} \sqrt{2}\left(\sigma_{11}x_{i_1}\right) + \mu_1, \\ \sqrt{2}\left(\sigma_{21}x_{i_1} + \sigma_{22}x_{i_2}\right) + \mu_2, \\ \ldots \\ \sqrt{2}\left(\sigma_{11}x_{i_1} + \cdots + \sigma_{nn}x_{i_n}\right) + \mu_n \end{pmatrix}$$

with μ_i as elements of the vector of expectations, and σ_{11},σ_{22},$\ldots$ as elements of the $\boldsymbol{\sigma}$ matrix.

With this in mind, it becomes trivial to evaluate the expectation terms in (20) using the following steps:

1. Draw m weights and nodes from a uni-variate GH quadrature as w_{i_j} and x_{i_j} where $i = 1, \ldots, m$ is the index of the quadrature points. The index j of the respective risk factor[12] will come into play in the next step.

2. Construct in a $m \times n$ matrix the Cartesian product of n copies of the univariate GH nodes form step (1). Each row of this matrix represents the transposed $\boldsymbol{x}_i$ quadrature node vector defined earlier. Denote by $\boldsymbol{z}_{1_j,2_j,\ldots,m_j} = \begin{pmatrix} x_{1_j}, & x_{2_j}, & \ldots, & x_{m,j} \end{pmatrix}'$ the j-th column from that matrix.

3. Similarly, construct the Cartesian product of n copies of the univariate GH weights form step (1). This produces the weights w_{j_k} needed in Equation (21).

4. In the discretized dynamic Equation (18) set $\Delta Z_{j,t} \equiv \sqrt{2}\boldsymbol{z}_{1_j,2_j,\ldots,m_j}$ for each $\Delta Z_{j,t}$ being an element of the vector of discretized Brownian motions $\boldsymbol{\Delta Z_t}$ and evaluate

[11] Here we assume that the same number m of nodes is used to evaluate each risk factor. In general, this need not be the case, and different number of nodes could be drawn for each risk factor.

[12] Which in our case corresponds to dZ_j, or the j-th element of the multivariate Brownian motion vector $\boldsymbol{dZ}$.

the gross return of the liuqid and corresponding the illiquid wealth. This produces an $m \times 1$ vector of returns for each wealth process, evaluated at the corresponding multivariate quadrature nodes.

5. Evaluate $R_{q,t+\Delta t}, \xi_{t+\Delta t}$ and $H(\xi_{t+\Delta t})$ at each node j.

6. Finally, evaluate the expectations terms in Equation 20 through the quadrature approximation defined in (21).

Online Annex:

B Benchmark Liquid Market: The Merton Model

B.1 Optimization

First, consider the benchmark case where all assets can be continuously traded. A representative investor holds a liquid financial portfolio out of which she can withdraw (consume) continuously the rate c_t. The investor has control over the asset allocation by setting the risky asset investment proportions collected in the column vector $\boldsymbol{\pi}_t$.[13] The wealth dynamics are then determined by the return of the portfolio net of the consumption rate:

$$\frac{dW_t}{W_t} = (r + \boldsymbol{\pi}_t'(\boldsymbol{\mu} - r\mathbb{1}) - c_t)dt + \boldsymbol{\pi}_t'\boldsymbol{\sigma}\boldsymbol{dZ}_t \tag{22}$$

Subject to these wealth dynamics, the investor optimizes over time her expected lifetime utility:

$$V(W_t) = \sup_{(\pi_s, C_s)} E_t \int_t^\infty \mathrm{e}^{-\beta(s-t)} u(C_s) ds \tag{23}$$

giving rise to the indirect utility of wealth function $V(W_t)$, with β a subjective discount rate, and $t \leq s$.

Applying the Bellman principle, we can derive the Hamilton-Jacobi-Bellman (HJB) equation:

$$\begin{aligned} &\mathcal{L}^C + \mathcal{L}^\pi - \beta V = 0 \\ &\mathcal{L}^C = \sup_{C_t} \left\{ u(C_t) - C_t V_W \right\} \\ &\mathcal{L}^\pi = \sup_{\boldsymbol{\pi}_t} \left\{ \left(r + \boldsymbol{\pi}_t'(\mu - r\mathbb{1})\right) V_W W_t + \frac{1}{2} V_{WW} W_t^2 \boldsymbol{\pi}_t' \boldsymbol{\Sigma} \boldsymbol{\pi}_t \right\} \end{aligned} \tag{24}$$

[13] More generally, $\boldsymbol{\pi}_t$ can be interpreted as exposures to factor excess returns.

where V_W and V_{WW} are the first- and second-order partial derivatives of the value function with respect to wealth.

Through a guess and verify strategy (cf. Annex B.3), the value function can then be determined in closed form as

$$V(W_t) = \left(\frac{1}{c}\right)^{\gamma} \frac{W_t^{1-\gamma}}{1-\gamma} \tag{25}$$

where $c = C_t/W_t$ is the optimal consumption rate which can be shown to be fixed over time and given by

$$c = \frac{\beta + r(\gamma - 1)}{\gamma} + \frac{1}{2}\frac{\gamma - 1}{\gamma^2}\|\boldsymbol{\lambda}\|^2 \tag{26}$$

In this setting, the investor can trade continuously and thus can always keep allocations at these base levels. Optimizing over $\boldsymbol{\pi}$ provides the optimal asset allocation vector:

$$\boldsymbol{\pi} = -\frac{V_W}{W_t V_{WW}}\boldsymbol{\Sigma}^{-1}(\boldsymbol{\mu} - \boldsymbol{r}\mathbb{1}) = \frac{1}{\gamma}(\boldsymbol{\sigma}')^{-1}\boldsymbol{\lambda} \tag{27}$$

The fraction $-\frac{V_W}{WV_{WW}} = \frac{1}{\gamma}$ defines the investor's relative risk tolerance given an indirect utility $V(W)$. The optimal risky allocation then is determined through the interaction of the investor's risk tolerance with the price of risk of each specific asset in the investment universe.

B.2 The HJB equation and optimal solution

In order to derive the continuous-time Bellman equation, we examine the value function defined in (23) over a short time period Δt. Assuming that the strategies for $\boldsymbol{\pi}_s$ and C_s are set in advance and stay constant for the time interval $s \in [t, t+\Delta t)$, and applying the Bellman principle of optimality, we can split today's value function into an optimizing

decision over the upcoming time span (from t until $t + \Delta t$) and an optimal strategy afterwards:

$$V(W_t) = \sup_{(\boldsymbol{\pi}_s, C_s)} \left\{ \int_t^{t+\Delta t} \mathrm{e}^{-\beta(s-t)} u(C_s) ds \right\} + \mathrm{e}^{-\beta \Delta t} E[V(t + \Delta t, W_{t+\Delta t})] \tag{28}$$

Note that the time subscript from the expectation has been dropped, as the wealth dynamics are driven by independent random shocks, implying that knowledge of the present does not help in forecasting the expected value function, so the unconditional expectation can be used instead of the conditional.

Multiplying both sides by $\frac{1}{\Delta t}\mathrm{e}^{\beta \Delta t}$ and rearranging:

$$\frac{\mathrm{e}^{\beta \Delta t} - 1}{\Delta t} V(W_t) = \sup_{(\boldsymbol{\pi}_s, C_s)} \frac{1}{\Delta t} \left\{ \int_t^{t+\Delta t} \mathrm{e}^{-\beta(s-t-\Delta t)} u(C_s) ds \right\} + \frac{1}{\Delta t} E\Big[V(W_{t+\Delta t}) - V(W_t) \Big]$$

We can evaluate the above equation for $\Delta t \to 0$. First, the by L'Hopital rule we have that $\lim_{\Delta \to 0} \frac{e^{\beta \Delta t - 1}}{\Delta t} = \beta$. Second, $\lim_{\Delta \to 0} \frac{1}{\Delta t} \int_t^{t+\Delta t} f(s) ds = f(t)$. Using the definition of a drift term in a stochastic differential equation by denoting it as $E[dV(t, W_t]$ we get the continuous time Bellman equation as

$$\beta V(t, W_t) = \sup_{(\boldsymbol{\pi}_t, C_t)} \{u(C_t)\} + E\Big[dV(t, W_t) \Big] \tag{29}$$

Apply the Itô rule on the stochastic term $dV(t, W_t)$ in (29) and substitute in the budget constraint for dW_t

$$\begin{aligned} dV &= V_W dW_t + 1/2 V_{WW} [dW_t]^2 \\ &= -C_t V_W dt + V_W W_t (r dt + \boldsymbol{\pi}_t' (\boldsymbol{\mu} - r \mathbb{1}) dt + \boldsymbol{\pi}_t' \boldsymbol{\sigma} \boldsymbol{dZ}_t) + \frac{1}{2} V_{WW} W^2 \boldsymbol{\pi}_t' \boldsymbol{\Sigma} \boldsymbol{\pi}_t dt \end{aligned}$$

Using the fact that $E[\boldsymbol{dZ}] = \mathbf{0}$ we can derive the drift term of the Bellman equation as

$$E\left[dV(t, W_t)\right] dt = \left[-C_t V_W + V_W W_t(r + \boldsymbol{\pi}_t'(\boldsymbol{\mu} - r\mathbb{1})) + \frac{1}{2} V_{ww} W^2 \boldsymbol{\pi}_t' \boldsymbol{\Sigma} \boldsymbol{\pi}_t\right] dt$$

which after substitution yields the HJB equation of Proposition (32):

$$\beta V(t, W_t) = \sup_{(\boldsymbol{\pi}_t, C_t)} u(C_t) - C_t V_W + V_W W_t(r + \boldsymbol{\pi}_t'(\boldsymbol{\mu} - r\mathbb{1})) + \frac{1}{2} V_{ww} W^2 \boldsymbol{\pi}_t' \boldsymbol{\Sigma} \boldsymbol{\pi}_t$$

B.3 Solving for the value function

We are using the verification approach for solving the HJB equation. This involves first solving the optimization part and finding the optimal $\boldsymbol{\pi}$ and C with the yet unknown value function.As a second step, we solve the resulting HJB equation by making a guess for the value function.

We can derive optimal consumption as:

$$\begin{aligned} u'(C_t) &= V_W \\ \implies C_t &= (V_W)^{-\frac{1}{\gamma}} \end{aligned} \tag{30}$$

This is the Envelope Theorem, implying that at optimality the marginal utility from consuming a little more needs to be the same as the marginal value of investing a little more.

Similarly, the optimal allocation is

$$\boldsymbol{\pi} = -\frac{V_W}{W_t V_{WW}} (\boldsymbol{\sigma}')^{-1} \boldsymbol{\lambda} \tag{31}$$

Substituting the optimal consumption and allocation terms, (30) and (31), in (24)

simplifies the HJB equation to:

$$\beta V = \frac{\gamma}{1-\gamma} V_W^{1-1/\gamma} + r W_t V_W - \frac{1}{2} \frac{V_W^2}{V_{WW}} \|\boldsymbol{\lambda}\|^2 \tag{32}$$

where $\|.\|^2$ represents the norm of a vector.

This second order Partial Differential Equation can be solved by making a guess for the value function of the form

$$V(W_t, t) = g(t)^\gamma \frac{W_t^{1-\gamma}}{1-\gamma}$$

Substituting in (32) verifies that the guess solves the PDE for $g(t) = \frac{1}{A}$, where

$$\begin{aligned} A &\equiv \frac{\beta + r(\gamma-1)}{\gamma} + \frac{1}{2}\frac{\gamma-1}{\gamma^2}\|\boldsymbol{\lambda}\|^2 \\ &= \frac{\beta + r(\gamma-1)}{\gamma} + \frac{1}{2}\frac{\gamma-1}{\gamma^2}(\boldsymbol{\mu} - r\mathbf{1})'(\boldsymbol{\sigma}\boldsymbol{\sigma}')^{-1}(\boldsymbol{\mu} - r\mathbf{1}) \end{aligned} \tag{33}$$

The optimal consumption share is thus

$$c = \frac{C_t}{W_t} = \frac{u'(V_W)^{-1}}{W_t} = A$$

where we make use of the Envelope Theorem in Equation (30), and $u'(.)^{-1}$ indicates the inverse function of the first derivative of $u(.)$. Note that $g(t)$ is a constant function. In the finite horizon case, it will be a deterministic function of time.

C Dynamic Model with Illiquidity: Proofs and Derivations

C.1 Illiquid market: Homogeneity of the value function

The proof follows from Ang et al. (2014). For CRRA utility in particular, the value function $V(W_t, X_t)$ is homogeneous of degree $1-\gamma$, such that $V(kW_t, kX_t) = k^{1-\gamma}V(W_t, X_t)$ for any $k > 0$. This is a direct consequence of the fact that the budget constraint dynamics are linear in wealth and have constant moments, independent of the corresponding wealth states. Then, it is reasonable to accept that for an optimal solution $\{W_s^*, X_s^*, dI_s^*, c_s^*, \theta_s^*\}$ also $\{kW_s^*, kX_s^*, kdI_s^*, c_s^*, \theta_s^*\}$ will be optimal as well for any $k > 0$, so that scaling both liquid and illiquid wealth up or down by the same number does not change the optimal investment and consumption rates given that we also scale the wealth transfers dI by the same number. As a result, we can write

$$V(kW_t, kX_t) = \sup_{\theta, dI, c} E_t \left[\int_t^\infty \mathrm{e}^{-\beta(s-t)} \frac{(kc_s(1-\xi_s)W_s)^{1-\gamma}}{1-\gamma} ds \right] = k^{1-\gamma}V(W_t, X_t)$$
$$\iff V(W_t, X_t) = \left(\frac{1}{k}\right)^{1-\gamma} V(kW_t, kX_t)$$

Then, setting $k = 1/(W_t + X_t)$ we get

$$V(W_t, X_t) = (X_t + W_t)^{1-\gamma} V\left((1-\xi), \xi\right) = (X_t + W_t)^{1-\gamma} H(\xi)$$

where ξ is the portion of total wealth invested in the illiquid asset x and $(1-\xi)$ is the portion invested in the liquid asset. The additional proof that $H(\xi)$ is concave is available in (Ang et al., 2014).

C.2 Deriving the HJB equation: One illiquid asset

Here we derive the HJB equation for the illiquid-asset problem, starting with the continuous time Bellman equation established in (29):

$$\beta V(X_t, W_t) = \sup_{(\xi_t, \theta_t, C_t)} \{u(C_t) + E[dV(X_t, W_t)]\}$$

Making use of the Ito rule for jump processes, we can write the drift of the equation as:

$$E[dV] = E\left[V_w dW^c + V_X dX^c + \frac{1}{2}\left(V_{WW}[dW^c]^2 + V_{XX}[dX^c]^2 + 2V_{WX}[dX^c dW^c]\right) + (V^* - V)dN\right]$$

where we denote as dX^c and dW^c the continuous portion of the wealth dynamics. Using the Ito rule, then we get the corresponding quadratic variation terms:

$$[dW_t^c]^2 = W_t^2 \boldsymbol{\theta}_t' \boldsymbol{\sigma}_w \boldsymbol{\sigma}_w' \boldsymbol{\theta}_t dt$$
$$[dX_t^c]^2 = X_t^2 \boldsymbol{\sigma}_x \boldsymbol{\sigma}_x' dt$$
$$[dW_t^c dX_t^c] = W_t X_t \boldsymbol{\theta}_t' \boldsymbol{\sigma}_w \boldsymbol{\sigma}_x' dt$$

since we know that

$$dW_t^c = W_t^c\left((r + \boldsymbol{\theta}_t'(\boldsymbol{\mu}_w - r\mathbb{1}) - c_t)dt + \boldsymbol{\theta}_t' \boldsymbol{\sigma}_w \boldsymbol{dZ}\right)$$
$$dX_t^c = X_t^c\left(\mu_x dt + \boldsymbol{\sigma}_x \boldsymbol{dZ}_t\right)$$

and denoting the jump size in the value function when a liquidity opportunity arises as $V^* - V(W_t, X_t)$, such that the expected jump size over a short period of time is $\eta(V^* - V(W_t, X_t))dt$. Note that whenever the Poisson jump process hits, we have inferred that the value function jumps to $V^* = (W_t + X_t)^{1-\gamma} H^*$.

This yields the given HJB equation

$$\mathcal{L}^C + \mathcal{L}^\theta + \mathcal{L} - \beta V(W_t, X_t) = 0$$

where

$$\begin{aligned}
\mathcal{L}^C &= \sup_{C_t} \left\{ u(C_t) - C_t V_W \right\} \\
\mathcal{L}^\theta &= \sup_{\theta_t} \left\{ (r + \boldsymbol{\theta}_t'(\boldsymbol{\mu}_w - r\mathbb{1})V_W W_t + \frac{1}{2} V_{WW} W_t^2 \boldsymbol{\theta}_t' \boldsymbol{\sigma}_w \boldsymbol{\sigma}_w' \boldsymbol{\theta}_t + V_{WX} W_t X_t \boldsymbol{\theta}_t' \boldsymbol{\sigma}_w \boldsymbol{\sigma}_x' \right\} \\
\mathcal{L} &= V_X \mu_x + \frac{1}{2} V_{XX} X^2 \boldsymbol{\sigma}_x \boldsymbol{\sigma}_x' + \eta \left(V^* - V(W_t, X_t) \right)
\end{aligned}$$

To rewrite the HJB equation in terms of ξ and $H(\xi)$ we use the following:

$$\begin{aligned}
\xi_t &= \frac{X_t}{W_t + X_t} \\
V(W_t, X_t) &= (W_t + X_t)^{1-\gamma} H(\xi_t)
\end{aligned}$$

such that

$$\begin{aligned}
V_W &= (W + X)^{-\gamma} \left((1-\gamma)H(\xi) - \xi H'(\xi) \right) \\
V_X &= (W + X)^{-\gamma} \left((1-\gamma)H(\xi) + (1-\xi)H'(\xi) \right) \\
V_{WW} &= (W + X)^{-\gamma-1} \left(-\gamma(1-\gamma)H(\xi) + 2\xi\gamma H'(\xi) + \xi^2 H''(\xi) \right) \\
V_{XX} &= (W + X)^{-\gamma-1} \left(-\gamma(1-\gamma)H(\xi) - 2(1-\xi)\gamma H'(\xi) + (1-\xi)^2 H''(\xi) \right) \\
V_{WX} &= (W + X)^{-\gamma-1} \left(-\gamma(1-\gamma)H(\xi) - 2(1-\xi)\gamma H'(\xi) - (1-\xi)H''(\xi)\xi \right)
\end{aligned}$$

The partial derivatives are implied using the Chain Rule such that $\frac{\partial \xi}{\partial X} = \frac{1-\xi}{W+X}$ and $\frac{\partial \xi}{\partial W} = -\frac{\xi}{W+X}$, where $H'(\xi_t)$ and $H''(\xi_t)$ denote the first and second partial derivatives of

$H(\xi)$ with respect to ξ.

Then we have the consumption term $\mathcal{L}^C$

We use $C_t = c_t W_t = c_t(1-\xi)Q_t$:

$$\begin{aligned}
\mathcal{L}^C &= \sup_{c_t}\left\{\frac{[c_t(1-\xi)Q_t]^{1-\gamma}}{1-\gamma} - c_t(1-\xi)Q_t\cdot V_W\right\} \\
&= Q_t^{1-\gamma}(1-\xi)^{1-\gamma}\cdot\sup_{c_t}\left\{\frac{c_t^{1-\gamma}}{1-\gamma} - c_t\left((1-\gamma)H(\xi)-\xi H'(\xi)\right)\right\} \qquad (34)\\
&\equiv Q_t^{1-\gamma}\cdot\tilde{\mathcal{L}}^C(\xi) \qquad (35)
\end{aligned}$$

The portfolio term $\mathcal{L}^\theta$ is

$$\begin{aligned}
\mathcal{L}^\theta &= \sup_{\theta_t}\left\{W_t\cdot(r+\boldsymbol{\theta}_t'(\boldsymbol{\mu}_w - r\mathbb{1}))V_W + \frac{1}{2}V_{WW}W_t^2\boldsymbol{\theta}_t'\boldsymbol{\Sigma}_w\boldsymbol{\theta}_t + V_{WX}W_tX_t\boldsymbol{\theta}_t'\boldsymbol{\sigma}_w\boldsymbol{\sigma}_x'\right\} \\
&= Q_t^{1-\gamma}\cdot\sup_{\theta_t}\Bigg\{(1-\xi)\left((1-\gamma)H(\xi)-\xi H'(\xi)\right)\cdot\boldsymbol{\theta}_t'(\boldsymbol{\mu}_w - r\mathbb{1}) \qquad (36)\\
&\quad + \frac{1}{2}(1-\xi)^2\left(-\gamma(1-\gamma)H(\xi)+2\xi\gamma H'(\xi)+\xi^2H''(\xi)\right)\boldsymbol{\theta}_t'\boldsymbol{\Sigma}_w\boldsymbol{\theta}_t \\
&\quad + \xi(1-\xi)\left(-\gamma(1-\gamma)H(\xi)-2(1-\xi)\gamma H'(\xi)-\xi(1-\xi)H''(\xi)\right)\boldsymbol{\theta}_t'\boldsymbol{\sigma}_w\boldsymbol{\sigma}_x'\Bigg\} \\
&\equiv Q_t^{1-\gamma}\cdot\tilde{\mathcal{L}}^\theta(\xi) \qquad (37)
\end{aligned}$$

The illiquid asset term $\mathcal{L}$ is derived as

$$\begin{aligned}
\mathcal{L} &= V_X\mu_x + \frac{1}{2}V_{XX}X^2\boldsymbol{\sigma}_x\boldsymbol{\sigma}_x' + \eta(V^*-V) \\
&= Q_t^{1-\gamma}\cdot\Big[\left((1-\gamma)H(\xi)+(1-\xi)H'(\xi)\right)\mu_x \qquad (38)\\
&\quad + \frac{1}{2}\xi^2\left(-\gamma(1-\gamma)H(\xi)-2(1-\xi)\gamma H'(\xi)+(1-\xi)^2H''(\xi)\right)\boldsymbol{\sigma}_x\boldsymbol{\sigma}_x'\Big] + \eta\left(V^* - Q_t^{1-\gamma}H(\xi)\right) \\
&\equiv Q_t^{1-\gamma}\cdot\tilde{\mathcal{L}}(\xi) + \eta Q_t^{1-\gamma}\left(H^* - H(\xi)\right) \qquad (39)
\end{aligned}$$

Combining the terms:

$$Q_t^{1-\gamma}\left[\tilde{\mathcal{L}}^C(\xi)+\tilde{\mathcal{L}}^\theta(\xi)+\tilde{\mathcal{L}}(\xi)-\beta H(\xi)\right]+\eta\left(V^*-Q_t^{1-\gamma}H(\xi)\right)=0 \tag{40}$$

Dividing through by $Q_t^{1-\gamma}$, we get the reduced-form equation in $H(\xi)$:

$$\tilde{\mathcal{L}}^C(\xi)+\tilde{\mathcal{L}}^\theta(\xi)+\tilde{\mathcal{L}}(\xi)-\beta H(\xi)+\eta\left(H^*-H(\xi)\right)=0 \tag{41}$$

Substituting these in the HJB equation we can solve for optimal consumption

$$c_t^*=\Big((1-\gamma)H(\xi_t)-H'(\xi_t)\xi_t\Big)^{-\frac{1}{\gamma}}(1-\xi_t)^{-1}$$

and optimal liquid risk asset investment

$$\theta_t^*=-\frac{k_1H(\xi_t)+k_2H'(\xi_t)+k_3H''(\xi_t)}{k_4H(\xi_t)+k_5H'(\xi_t)+k_6H''(\xi_t)}$$

where $k_1,..,k_6$ are known constants defined by the market parameters and the investor's risk aversion such that

$$\begin{aligned}
k_1&=-(1-\gamma)(\mu_1-r)+\gamma(1-\gamma)\sigma_2\rho\sigma_1\xi\\
k_2&=(\mu_1-r)\xi-\sigma_2\sigma_1\rho\xi\gamma(2\xi-1)\\
k_3&=-\sigma_2\sigma_1\rho\xi^2(1-\xi)\\
k_4&=-\gamma(1-\gamma)(1-\xi)\sigma_1^2\\
k_5&=2\gamma\xi(1-\xi)\sigma_1^2\\
k_6&=\xi^2(1-\xi)\sigma_1^2
\end{aligned}$$

Note that this also implies that investment and hedging curvature terms ($\Phi(\xi)$ and

respectively $\Psi(\xi)$ in (10)) can be written as a function of ξ_t such that:

$$\Phi(\xi) = \left(-\frac{V_W}{V_{WW}W_t}\right) = \frac{1}{1-\xi}\left(\frac{(1-\gamma)H(\xi) - \xi H'(\xi)}{-\gamma(1-\gamma)H(\xi) - 2(1-\xi)\gamma H'(\xi) + (1-\xi)^2 H''(\xi)}\right)$$
$$\Psi(\xi_t) = -\frac{V_{WX}X_t}{V_{WW}W_t} = \frac{-\gamma(1-\gamma)H(\xi) - 2(1-\xi)\gamma H'(\xi) - (1-\xi)H''(\xi)\xi}{-\gamma(1-\gamma)H(\xi) - 2(1-\xi)\gamma H'(\xi) + (1-\xi)^2 H''(\xi)}$$